Evidence for Intramolecular N−H···O Resonance-Assisted Hydrogen Bonding in β-Enaminones and Related Heterodienes. A Combined Crystal-Structural, IR and NMR Spectroscopic, and Quantum-Mechanical Investigation

Paola Gilli, Valerio Bertolasi, Valeria Ferretti, and Gastone Gilli*

Contribution from the Centro di Strutturistica Diffrattometrica and Dipartimento di Chimica, Università di Ferrara, 44100 Ferrara, Italy

Received March 14, 2000

Abstract: The resonance-assisted hydrogen bond (RAHB) is a model of synergistic interplay between π-delocalization and hydrogen-bond (H-bond) strengthening originally introduced (Gilli, G.; Bellucci, F.; Ferretti, V.; Bertolasi, V. *J. Am. Chem. Soc.* **1989**, *111*, 1023; Bertolasi, V.; Gilli, P.; Ferretti, V.; Gilli, G. *J. Am. Chem. Soc.* **1991**, *113*, 4917) for explaining the abnormally strong intramolecular O−H···O bonds formed by the ···O=C−C=C−OH··· β-enolone fragment **I** which are typical of β-diketone enols. The applicability of this model to the intramolecular N−H···O hydrogen bonds formed by a number of heteroconjugated systems (···O=C−C=C−NH···, β-enaminones **II**; ···O=C−C=N−NH···, ketohydrazones **III**; and ···O=N−C=C−NH···, nitrosoenamines **IV**) is investigated. The X-ray crystal structures of five molecules which close a six-membered ring by an intramolecular N−H···O bond through the resonant ···O=X−C=X−NH··· (X = C, N) fragments **II**−**IV** are compared to those of two other molecules closing the same ring through the nonresonant ···O=C−C−C−NH··· β-aminone moiety **V**. Experimental findings are complemented by a CSD (Cambridge Structural Database) search of all compounds forming intramolecular N−H···O bonds through the molecular fragments **II**−**V** and by a comprehensive analysis of the IR ν_{NH} stretching frequencies and ^{1}H NMR δ_{NH} chemical shifts available for compounds of these classes of known crystal structure. It is shown that all the descriptors of H-bond strength [d(N···O) shorthening, decrease of ν_{NH}, increase of δ_{NH}, and increase of π-delocalization within the heteroconjugated fragment] are mutually intercorrelated according to RAHB rules, which can then account for the strength of heteronuclear N−H···O bonds in **II**−**IV** as well as for that of the homonuclear O−H···O bonds in **I**. Heteronuclear N−H···O bonds appear, however, to have distinctive features. In particular, their strength turns out to be partially hampered by the proton affinity difference (ΔPA) between the N and O atoms, so that very strong H-bonds (2.65 $\geq$ d(N···O) $\geq$ 2.48 Å, 3200 $\geq$ ν_{NH} $\geq$ 2340 cm^{-1}, 13 $\leq$ δ_{NH} $\leq$ 18 ppm) can occur only when the π-delocalization of the heterodienic moiety is associated with proper electron-attracting substituents which are able to decrease this ΔPA by increasing the NH acidity. Moreover, at variance with strong O−H···O RAHBs, whose protons are mostly found in nearly symmetrical positions, even the strongest N−H···O RAHBs are highly dissymmetric, despite the very similar changes undergone by both IR and ^{1}H NMR spectra in O−H···O and N−H···O H-bonded systems. Specificities of heteronuclear H-bonds are shown to be interpretable by the electrostatic-covalent H-bond model (ECHBM) which was previously developed for the homonuclear case (Gilli, P.; Bertolasi, V.; Ferretti, V.; Gilli, G. *J. Am. Chem. Soc.* **1994**, *116*, 909). The conclusions drawn are corroborated by extended DFT quantum-mechanical calculations at the B3LYP/6-31+G(d,p)//B3LYP/6-31+G(d,p) level of theory and by full geometry optimization carried out on 27 variously substituted heterodienes **II**−**IV** and nonresonant β-aminones **V**. Calculations allow the estimation of H-bond energies that are found to be approximately 2.75 kcal mol^{-1} for nonresonant **V** and 5.22, 6.12, and 7.03 kcal mol^{-1} for unsubstituted resonant **II**, **III**, and **IV**, respectively. Proper substitutions of β-enaminone **II** nearly double H-bond energies, making them comparable to those calculated for homonuclear O−H···O RAHB in β-diketone enols (9.51 and 13.08 kcal mol^{-1} for malondialdehyde and acetylacetone, respectively).

Introduction

Many books of elementary chemistry still describe the hydrogen bond (H-bond) as a weak, secondary interaction of a few kcal mol^{-1}, differing from van der Waals or multipolar interactions mainly because of its greater directionality, while the few cases of very strong H-bonds are treated as peculiarities of some elements (e.g. fluorine). In the last few decades it has become increasingly clear, thanks to the accurate reviews by Speakman,[1a] Huggins,[1b] Emsley,[1c] and Jeffrey[1d−f] and the renewed interest in strong low-barrier H-bonds (LBHB),[2] that there are too many cases of "abnormally" strong H-bonds to consider them as separate anomalies and that a new general classification of strong, as well as weak, H-bonds is needed.

The first comprehensive classification of homonuclear O−H···O bonds, inclusive of very strong ones, is due to Gilli

* To whom correspondence should be addressed: Dipartimento di Chimica, Università di Ferrara, Via L. Borsari, 46, 44100 Ferrara, Italy. Tel: +39-0532-291141. Fax: +39-0532-240709. E-mail: ggilli.chim@unife.it.

10.1021/ja000921+ CCC: $19.00
Published on Web 10/06/2000

and co-workers,[3a] who suggested, on the grounds of a large neutron and X-ray crystal-structure evidence, that there can only be (A) three classes of really strong H-bonds: (i) (−)CAHB: $[O\cdots H\cdots O]^-$, negative-charge-assisted H-bonds; (ii) (+)-CAHB: $[O\cdots H\cdots O]^+$, positive-charge-assisted H-bonds; and (iii) RAHB: $-O-H\cdots O=$, resonance-assisted H-bonds[3b,c], or π-cooperative H-bonds[1d], where the two oxygen atoms are connected by a π-conjugated system of single and double bonds; (B) one class of moderate H-bonds: PAHB, consisting of $\cdots O-H\cdots O-H\cdots$ chains of polarization-assisted, or σ-cooperative[1d], H-bonds; and (C) one overall class of weak, isolated H-bonds (IHB), which are characterized by being neither charged nor σ- or π-cooperative. Typical (−)CAHBs [$2.3 \le d(O\cdots O) \le 2.50$ Å] are well-exemplified by intermolecular $[RCOOH\cdots OOCR]^-$ bonds between carboxylic acids and carboxylates, $[O_nXOH\cdots OXO_n]^-$ bonds between inorganic oxoacids and their conjugated bases, or by the very short intramolecular $[O\cdots H\cdots O]^-$ bond in hydrogen maleate. Most (+)CAHBs ($2.36 \le d(O\cdots O) \le 2.43$ Å) are reducible to two identical oxygenated molecules (H_2O, R_2O, Me_2SO, pyridine *N*-oxide, etc.) which are bridged by a proton donated by a strong acid. The most common cases of RAHB come from the strong $O-H\cdots O$ bonds ($2.39 \le d(O\cdots O) \le 2.55$ Å) formed by the heteroconjugated $\cdots O=C-C=C-OH\cdots$ β-diketone enol group *I*, for which a positive synergism between H-bond strengthening and increased π-delocalization of the heterodiene has been sometimes suggested in the past,[1b,4] but only recently has been described in detail for both intramolecular[3b−d] and intermolecular[3e−f] cases. More generally, all RAHBs can be reduced to the formula $\cdots A=R_n-DH\cdots$, where A and D are the H-bond donor and acceptor atoms, and R_n ($n = 1,3,5,7...$) is a resonant spacer of *n* atoms which form a chain of alternating single and double bonds[3g] (e.g.: $n = 1$ for carboxylic acids and amides, $n = 3$ for β-diketone enols and β-enaminones, and so on). Finally, examples of PAHB are found in ice, alcohol, and phenol crystal chemistry as well as in some inorganic acids such as boric acid[1e].

It has been shown that this classification can be generalized to all homonuclear $X-H\cdots X$ bonds and is consistent with what can be called the electrostatic-covalent H−bond model (ECHBM),[3a,h] that states that (a) weak H-bonds are electrostatic in nature but become increasingly covalent with increasing strength; (b) very strong H-bonds are essentially three-center-four-electron covalent bonds; (c) the strongest H-bonds must be homonuclear ($X-H\cdots X$) and symmetrical on the two sides of the H-bond, because only in this situation are the two VB resonance forms $X-H\cdots X \leftrightarrow X\cdots H-X$ isoenergetic and can they mix to the greatest extent; (d) this last condition can be more generally expressed[5,6] as a condition of minimum ΔPA (the proton affinity difference between the H-bond donor and the acceptor atoms) or of minimum ΔpK_a (the pK_a difference between the two interacting groups as measured in a proper polar solvent). The most controversial ECHBM assumption, that is, the covalent nature of very strong $O-H\cdots O$ bonds[3a], has been suggested by a number of different authors,[7] but has only recently received authoritative support by very accurate X−N electron-density measurements that identified a "covalent" (3,−1) critical point with negative Laplacian[8] along the $H\cdots O$ bond in both (−)CAHB[9a,b] and RAHB[9c,d] cases.

If possible, the heteronuclear $N-H\cdots O$ is even more important than the homonuclear $O-H\cdots O$ bond because of its outstanding importance in protein folding and DNA pairing and its ever-growing applications in molecular recognition and crystal engineering problems;[10] however, no systematic investigation of strong $N-H\cdots O$ bonds is available. To start with, the present paper reports the first general study of the resonance-assisted intramolecular $N-H\cdots O$ bond formed by the heterodienic fragments 1-en-1-amino-3-one (β-enaminone) **II**, 1-aza-β-enaminone (ketohydrazone) **III**, and 3-aza-β-enaminone (nitrosoenamine) **IV**, which have the correct geometry to form potentially strong $N-H\cdots O$ R_3-RAHBs which are similar to those formed by β-diketone enols (β-enolones) **I**.

(1) (a) Speakman, J. C. *Struct. Bond.* **1972**, *12*, 141. (b) Huggins, M. L. *Angew. Chem., Int. Ed. Engl.* **1971**, *10*, 147. (c) Emsley, J. *Chem. Soc. Rev.* **1980**, *9*, 91. (d) Jeffrey, G. A.; Saenger, W. *Hydrogen Bonding in Biological Structures*; Springer-Verlag: Berlin, 1991. (e) Jeffrey, G. A. *An Introduction to Hydrogen Bonding*; Oxford University Press: New York, 1997. (f) Jeffrey, G. A. *Cryst. Rev.* **1995**, *4*, 213.

(2) (a) Cleland, W. W. *Biochemistry* **1992**, *31*, 317. (b) Cleland, W. W.; Kreevoy, M. M. *Science* **1994**, *264*, 1887. (c) Cleland, W. W.; Frey, P. A.; Gerlt, J. A. *J. Biol. Chem.* **1998**, *273*, 25529. (d) Frey, P. A.; Whitt, S. A.; Tobin, J. B. *Science* **1994**, *264*, 1927. (e) Warshel, A.; Papazyan, A.; Kollman, P. A. *Science* **1995**, *269*, 102. (f) Shan, S.-o.; Loh, S.; Herschlag, D. *Science* **1996**, *272*, 97. (g) Shan, S.-o.; Herschlag, D. *Proc. Natl. Acad. Sci. U.S.A.* **1996**, *93*, 14474. (h) Harris, T. K.; Mildvan, A. S. *Proteins* **1999**, *35*, 275.

(3) (a) Gilli, P.; Bertolasi, V.; Ferretti, V.; Gilli, G. *J. Am. Chem. Soc.* **1994**, *116*, 909. (b) Gilli, G.; Bellucci, F.; Ferretti, V.; Bertolasi, V. *J. Am. Chem. Soc.* **1989**, *111*, 1023. (c) Bertolasi, V.; Gilli, P.; Ferretti, V.; Gilli, G. *J. Am. Chem. Soc.* **1991**, *113*, 4917. (d) Gilli, P.; Ferretti, V.; Bertolasi, V.; Gilli, G. In *Advances in Molecular Structure Research*; Hargittai, I., Hargittai, M., Eds.; JAI Press, Inc.: Greenwich, CT, 1996; Vol. 2, p 67. (e) Gilli, G.; Bertolasi, V.; Ferretti, V.; Gilli, P. *Acta Crystallogr.* **1993**, *B49*, 564. (f) Bertolasi, V.; Gilli, P.; Ferretti, V.; Gilli, G. *Chem. Eur. J.* **1996**, *2*, 925. (g) Gilli, P.; Ferretti, V.; Gilli, G. In *Fundamental Principles of Molecular Modeling*; Gans, W., Amann, A., Boeyens, J. C. A., Eds.; Plenum Press: New York, 1996. (h) Gilli, G.; Gilli, P. *J. Mol. Struct.* **2000**, *552*, 1.

(4) (a) Vinogradov, S. N.; Linnel, R. H. *Hydrogen Bonding*; Van Nostrand Reinhold: New York, 1971. (b) Haddon, R. C. *J. Am. Chem. Soc.* **1980**, *102*, 1807. (c) Emsley, J. *Struct. Bond.* **1984**, *57*, 147. (d) Kopteva, T. S.; Shigorin, D. N. *Russ. J. Phys. Chem.* **1974**, *48*, 312.

(5) (a) Meot-Ner (Mautner), M. *J. Am. Chem. Soc.* **1984**, *106*, 1257. (b) Meot-Ner (Mautner), M. In *Molecular Structure and Energetics*; Liebman, J. F., Greenberg, A., Eds.; VCH: Weinheim, 1987; Vol. IV, Chapter 3. (c) Zeegers-Huyskens, T.; Huyskens, P. L. In *Intermolecular Forces*; Huyskens, P. L., Luck, W. A., Zeegers-Huyskens, T., Eds.; Springer-Verlag: Berlin, 1991; Chapter 1. (d) Zeegers-Huyskens, T. *J. Org. Chem.* **1999**, *64*, 4946. (e) Chen, J.; McAllister, M. A.; Lee, J. K.; Houk, K. N. *J. Org. Chem.* **1998**, *63*, 4611. (f) Malarski, Z.; Rospenk, M.; Sobczyk, L.; Grech, E. *J. Phys. Chem.* **1982**, *86*, 401. (g) Zeegers-Huyskens, T. In *Intermolecular Forces*; Huyskens, P. L., Luck, W. A., Zeegers-Huyskens, T., Eds.; Springer-Verlag: Berlin, 1991; Chapter 6. (h) Sobczyk, L. *Ber. Bunsen-Ges. Phys. Chem.* **1998**, *102*, 377.

(6) The above discussion concerns only homonuclear $X-H\cdots X$ bonds. It has to be stressed, however, that the condition of minimum ΔPA or ΔpK_a can be applied to heteronuclear H-bonds as well, in particular to acid−base $O-H\cdots N \rightleftarrows O^-\cdots H-N^+$ bonds that can become very strong when either the ΔPA or the ΔpK_a approaches zero. See: Reinhardt, L. A.; Sacksteder, K. A.; Cleland, W. W. *J. Am. Chem. Soc.* **1998**, *120*, 13366, and refs 2 and 5f−h.

(7) (a) Coulson, C. A.; Danielsson, U. *Ark. Fys.* **1954**, *8*, 239. (b) Coulson, C. A.; Danielsson, U. *Ark. Fys.* **1954**, *8*, 245. (c) Pimentel, G. C. *J. Chem. Phys.* **1951**, *19*, 446. (d) Reid, C. *J. Chem. Phys.* **1959**, *30*, 182. (e) Kollman, P. A.; Allen, L. C. *J. Am. Chem. Soc.* **1970**, *92*, 6101. (f) Stevens, E. D.; Lehmann, M. S.; Coppens, P. *J. Am. Chem. Soc.* **1977**, *99*, 2829. (g) King, B. F.; Weinhold, F. *J. Chem. Phys.* **1995**, *103*, 333. (h) Dannenberg, J. J.; Haskamp, L.; Masunov, A. *J. Phys. Chem. A* **1999**, *103*, 7083.

(8) Bader, R. F. W. *Atoms in Molecules: a Quantum Theory*; Oxford University Press: New York, 1990.

(9) (a) Flensburg, C.; Larsen, S.; Stewart, R. F. *J. Phys. Chem.* **1995**, *99*, 10130. (b) Madsen, D.; Flensburg, C.; Larsen, S. *J. Phys. Chem. A* **1998**, *102*, 2177. (c) Madsen, G. K. H.; Iversen, B. B.; Larsen, F. K.; Kapon, M.; Reisner, G. M.; Herbstein, F. H. *J. Am. Chem. Soc.* **1998**, *120*, 10040. (d) Madsen, G. H. K. Personal communication, 1998.

(10) (a) Desiraju, G. R. *Crystal Engineering: The Design of Organic Solids*; Elsevier: Amsterdam, 1989. (b) *Molecular Recognition: Chemical and Biochemical Problems II*; Roberts, S. M., Ed.; The Royal Society of Chemistry: Cambridge, U.K., 1992. (c) Chemla, D. S.; Zyss, J. *Nonlinear Optical Properties of Organic Molecules and Crystals;* Academic Press: Orlando, FL, 1987; Vols. 1, 2. (*d*) MacDonald, J. C.; Whitesides, G. M. *Chem. Rev.* **1994**, *94*, 2383. (e) Etter, M. C. *J. Phys. Chem.* **1991**, *95*, 4601. (f) Bernstein, J.; Davis, R. E.; Shimoni, L.; Chang, N.-L. *Angew. Chem., Int. Ed. Engl.* **1995**, *34*, 1555. (g) Desiraju, G. R. *Angew. Chem., Int. Ed. Engl.* **1995**, *34*, 2311.

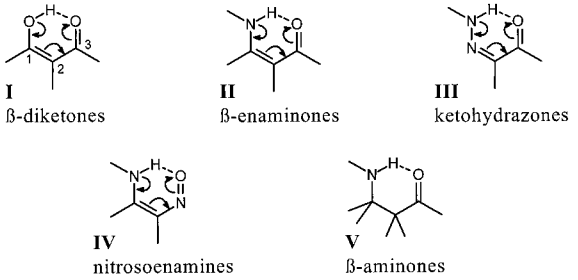

Previous investigations[11] of ketohydrazones **III** have shown that the intramolecular N−H···O bond may be remarkably strengthened, up to a N···O distance of 2.551 Å, by the addition of an electron-withdrawing carbonyl in position 2. To check whether similar substitution may also strengthen the H-bond in β-enaminones **II** and nitrosoenamines **IV**, we present here syntheses, crystal structures, and some relevant IR and NMR spectroscopic data of five 2-COOR-substituted derivatives, that is, the four β-enaminones **a**−**d** and the nitrosoenamine **e**. To assess the relative importance of resonance, the crystal structures of two β-aminones **V** which form a similar, but nonresonant, intramolecular H-bond (**f** and **g**) are also reported.

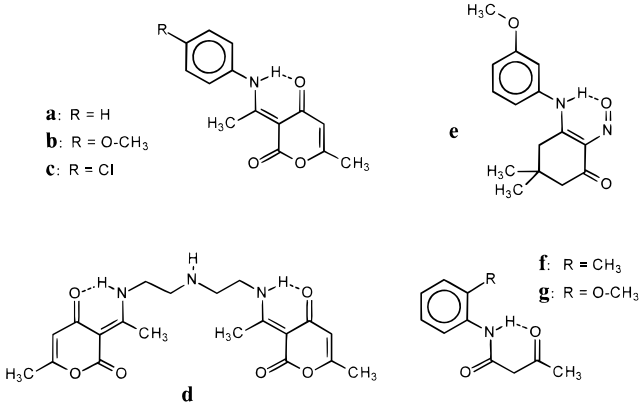

To put the results in a wider perspective, experimental data are integrated by a systematic search of the CSD files[12] for all crystals presenting the intramolecularly H-bonded O═X−C═X−NH (X = C or N) fragments **II**−**IV** and by a spectroscopic investigation of the relationships among N···O distances, δ_{NH} ^{1}H NMR chemical shifts, and ν_{NH} IR stretching frequencies of the proton involved in the H-bond formation. Finally, because structural and spectroscopic data cannot predict H-bond association energies, these are evaluated by comparing high-level quantum-mechanical calculations on selected model molecules in their H-bonded (closed) and non-H-bonded (open) forms.

Discussion

Analysis of Crystal Structures. Crystal structure determination details are given in the Experimental Section. ORTEP[13] views of the molecules with thermal ellipsoids at 40% probability are shown in Figure 1. Selected bond distances are reported in Table 1 and H-bond parameters, together with the measured IR ν_{NH} and ^{1}H NMR δ_{NH} values, in Table 2. Compounds **a**−**d** adopt the β-enaminone tautomeric form and display intramolecular H-bonds ($2.522 \le d(N\cdots O) \le 2.563$ Å) which are among the shortest intramolecular N−H···O bonds ever observed. These are associated with remarkable delocalizations of the O═C−C═C−NH π-conjugated β-enaminonic system, as shown by the comparison of the C═O, C−C, C═C

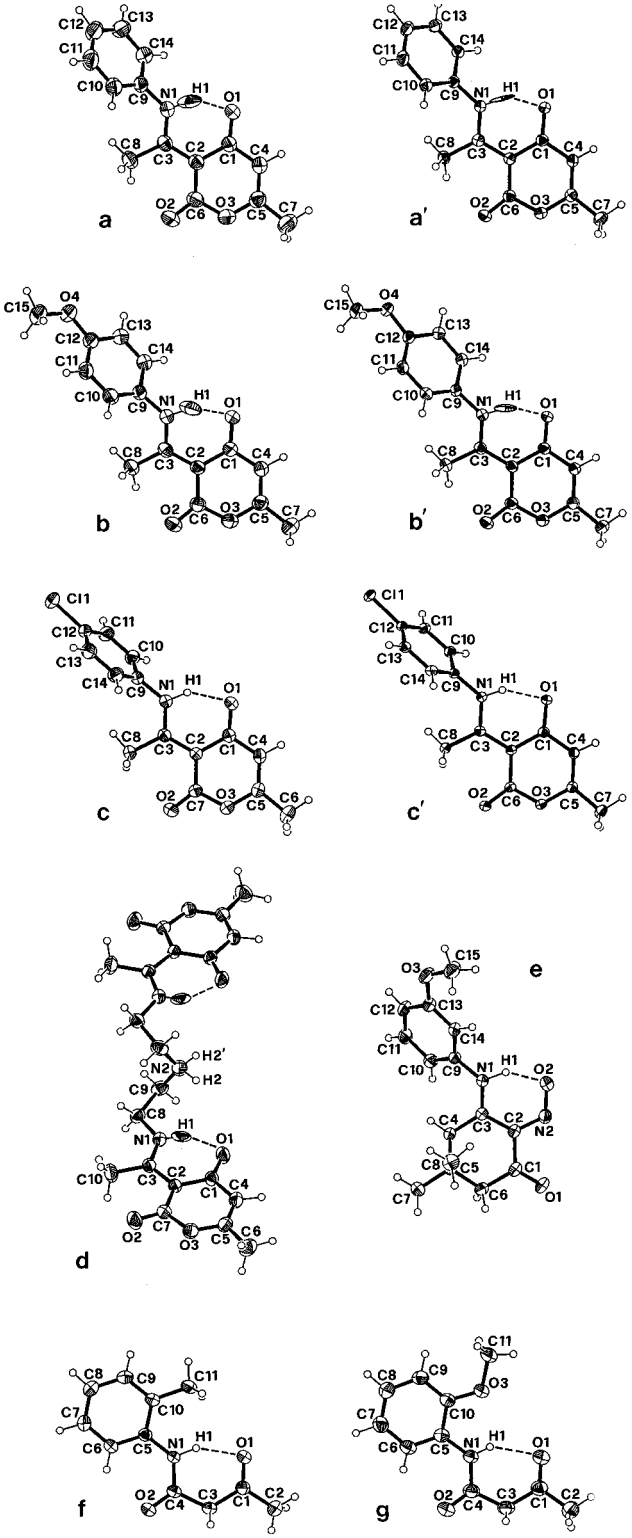

Figure 1. ORTEP[13] views of the crystal structures determined at room temperature (**a**−**g**) and at 150 K (**a′**−**c′**). Thermal ellipsoids drawn at 40% probability. Atoms H2 and H2′ of structure **d** are disordered around the 2-fold axis on which the N2 atom is located.

(11) (a) Bertolasi, V.; Ferretti, V.; Gilli, P.; Gilli, G.; Issa, Y. M.; Sherif, O. E. *J. Chem. Soc., Perkin Trans. 2* **1993**, 2223. (b) Bertolasi, V.; Nanni, L.; Gilli, G.; Ferretti, V.; Gilli, P.; Issa, Y. M.; Sherif, O. E. *New J. Chem.* **1994**, *18*, 251. (c) Bertolasi, V.; Gilli, P.; Ferretti, V.; Gilli, G.; Vaughan, K. *New J. Chem.* **1999**, *23*, 1261.

(12) Allen, F. H.; Bellard, S.; Brice, M. D.; Cartwright, B. A.; Doubleday, A.; Higgs, H.; Hummelink, T.; Hummelink-Peters, B. G.; Kennard, O.; Motherwell, W. D. S.; Rodgers, J.; Watson, D. G. *Acta Crystallogr*. **1979**, *B35*, 2331.

(13) Johnson, C. K. *ORTEPII*; Report ORNL-5138; Oak Ridge National Laboratory: Oak Ridge, TN, 1976.

Table 1. Selected Bond Distances (Å) for Compounds **a**−**g**

compd	C1−O1	C1−C2	C2−C3	N1−C3	C1−C4	C2−C6	C6−O2	C4−C5	C5−O3	O3−C6
a	1.257(1)	1.438(2)	1.422(2)	1.318(2)	1.439(2)	1.437(2)	1.208(2)	1.326(2)	1.361(2)	1.396(2)
a′	1.262(2)	1.445(2)	1.427(2)	1.322(2)	1.436(2)	1.438(2)	1.219(2)	1.330(2)	1.366(2)	1.397(2)
b	1.266(2)	1.437(2)	1.424(2)	1.319(2)	1.434(2)	1.440(2)	1.208(2)	1.326(3)	1.362(2)	1.393(2)
b′	1.264(2)	1.446(2)	1.427(2)	1.319(2)	1.438(2)	1.438(2)	1.212(2)	1.333(3)	1.365(2)	1.397(2)
c	1.251(2)	1.448(2)	1.420(2)	1.320(2)	1.437(2)	1.444(2)	1.200(2)	1.326(2)	1.364(2)	1.399(2)
c′	1.260(3)	1.449(3)	1.424(3)	1.325(3)	1.437(3)	1.446(3)	1.212(3)	1.332(3)	1.372(3)	1.398(2)
d	1.258(2)	1.445(2)	1.438(2)	1.303(2)	1.440(2)	1.431(2)	1.212(2)	1.330(2)	1.360(2)	1.398(2)
average	1.260[5]	1.444[4]	1.426[5]	1.318[6]	1.437[2]	1.439[4]	1.210[5]	1.329[3]	1.364[4]	1.397[2]

compd	N2−O2	N2−C2	C2−C3	N1−C3	C1−C2	C1−O1
e	1.288(2)	1.339(2)	1.438(2)	1.310(2)	1.478(2)	1.222(2)

compd	C1−O1	C1−C3	C3−C4	N1−C4	C4−O2
f	1.212(2)	1.507(2)	1.511(3)	1.349(2)	1.214(2)
g	1.211(2)	1.498(2)	1.508(2)	1.349(2)	1.212(2)
average	1.212[1]	1.502[4]	1.510[2]	1.349[1]	1.213[1]

Table 2. Geometric Parameters, IR ν_{NH}-Stretching Frequencies and ^{1}H NMR δ_{NH} Chemical Shifts for the Intramolecular N−H···O Hydrogen Bond in Compounds **a**−**g**

compd	N−H (Å)	N···O (Å)	H···O (Å)	N−H···O (deg)	ν_{NH} (cm^{-1})	δ_{NH} (ppm)
a	0.91(2)	2.522(2)	1.71(2)	147(2)	2612	15.82
a′	0.90(3)	2.526(2)	1.71(3)	148(2)		
b	0.97(2)	2.527(2)	1.65(1)	148(2)	2610	15.60
b′	0.94(3)	2.532(2)	1.67(2)	152(2)		
c	0.89(2)	2.531(2)	1.76(2)	143(2)	2602	15.90
c′	0.85(3)	2.536(2)	1.78(3)	147(3)		
d	0.84(2)	2.563(2)	1.83(2)	145(2)	2870	14.18
e	0.97(2)	2.516(2)	1.68(2)	142(2)	2560	18.41
f	0.94(2)	2.717(2)	1.89(2)	147(2)	3240	9.18
g	0.84(1)	2.748(2)	2.05(1)	141(1)	3281	9.24

and C−N distances (on average, 1.260[5], 1.444[4], 1.426[5] and 1.318[6] Å), with the corresponding pure double or single bond distances C(sp^2)═O ≃ 1.20, C(sp^2)−C(sp^2) ≃ 1.48, C(sp^2)═C(sp^2) ≃ 1.33,[14a] and C(sp^2)−N(sp^2) ≃ 1.44 Å.[14b] These geometric changes are paralleled by large ^{1}H NMR chemical shifts of 14.2−15.9 ppm (to be compared to 7−9 ppm for weak H-bonds) and red-shifted ν_{NH} stretching frequencies of 2602−2870 cm^{-1} (to be compared to about 3400 cm^{-1} for the free N−H). Because the β-enaminone moiety in **a**−**d** is fused with a similar pyrone ring, differences among the N···O contact distances are to be imputed, in addition to weak crystal field perturbations, to the effects of *N*-substitution. It was found that the presence of the more basic diethylenetriamine moiety in **d** induces a longer H-bond [d(N···O) = 2.563(2) Å] than does the presence of the less basic aniline group in **a**−**c** [d(N···O) = 2.52−2.53 Å], although no systematic effect of aniline *p*-substitution is detectable, which is at variance with what previously was found in diketoarylhydrazones.[11a,b] On the other hand, the importance of the pyrone ring in the shortening of the N−H···O bond seems indubitable, because the shortest N···O distance observed in simple β-enaminones (i.e. β-enaminones whose substituents are hydrogens and alkyl and aryl groups) is 2.602 Å.[14c] According to ECHBM rules, this shortening can be ascribed to the 2-carbonyl that, by π-conjugation, makes the N−H proton more acidic, thus reducing the ΔPA between H-bond donor and acceptor atoms, which is the preeminent cause of N−H···O bond weakening.

The average N−H···O angle of 147[3]° in **a**−**d** (Table 2) is comparable to the O−H···O angle of 149[5]° obtained as an average from a set of 99 β-diketone enols involved in the same intramolecular R$_3$−RAHB.[3d] No H-bond-induced lengthening of the N−H bond distance is, however, apparent. The average N−H distance is 0.90[4] Å, definitely shorter than the same distance if unperturbed by H-bonding (1.009 Å, as determined by neutron diffraction[14a] and 1.0116 Å, by gas-electron diffraction[14d]). Although too-short d(N−H) values are partially imputable to the fact that X-rays show average electron distributions and not nuclear positions, there is little doubt that the N−H lengthening due to strong N−H···O bond formation is irrelevant or very small, as already reported by other authors,[15a−c] and at variance with what has been observed in β-diketone enols, where d(O···O) values shorter than 2.45−2.50 Å are always associated with almost-centered protons having O−H distances as long as 1.25 Å.[3c] The problem of N−H lengthening will be further discussed in connection with IR and NMR results and quantum-mechanical calculations.

In analogy to the four β-enaminones **a**−**d**, the O═N−C═C−NH nitrosoenamine moiety in **e** displays O═N, N−C, C═C, and C−N distances which are strongly perturbed by π-delocalization effects, as shown by the experimental values of 1.288(2), 1.339(2), 1.438(2), and 1.310(2) Å, respectively, in comparison to the C═C and C−N values given above and with the pure double- and single-bond distances of 1.225 for N═O and 1.425 Å for ═N−OH which were derived from a comparative study of oximes and nitroso derivatives.[14e] In compound **e,** the N···O distance is as short as 2.516(2) Å, only longer than that of 2.483 Å which is found in another nitrosoenaminone[14e] that is chemically identical to **e** except for an *m*-methoxy substituent. It should be noted that both of these compounds share with **a**−**d** the carbonyl substituent in position 2, which has been confirmed as a H-bond strengthening group.

Compounds **f** and **g** form intramolecular N−H···O═C bonds by closing the nonresonant six-membered ring **V**, making it possible to evaluate the effects of π-conjugation removal from

(14) (a) Allen, F. H.; Kennard, O.; Watson, D. G.; Brammer, L.; Orpen, A. G.; Taylor, R. *J. Chem. Soc., Perkin Trans. 2* **1987**, S1. (b) Gilli, G.; Bertolasi, V.; Bellucci, F.; Ferretti, V. *J. Am. Chem. Soc.* **1986**, *108*, 2420. (c) Fernández-G., J. N.; Enriquez, R. G.; Tobón-Cervantes, A.; Bernal-Uruchurtu, M. I.; Villena-I., R.; Reynolds, W. F.; Yang, J.-P. *Can. J. Chem.* **1993**, *71*, 358. (d) Vilkov, L. V.; Sadova, N. I. In *Stereochemical Applications of Gas-Phase Electron Diffraction*; Hargittai, I., Hargittai, M., Eds.; VCH: Weinheim, 1988; Part B, p 35. (e) Gilli, G.; Bertolasi, V.; Veronese, A. C. *Acta Crystallogr.* **1983**, *B39*, 450.

(15) (a) Olovsson, I.; Jönsson, P.-G. In *The Hydrogen Bond. Recent Developments in Theory and Experiments*; Schuster, P., Zundel, G., Sandorfy, C., Eds.; North-Holland: Amsterdam, 1976; Vol. 2, Chapter 8. (b) Steiner, Th. *J. Phys. Chem. A* **1998**, *102*, 7041. (c) Overgaard, J.; Schiøtt, B.; Larsen, F. K.; Schultz, A. J.; MacDonald, J. C.; Iversen. B. B. *Angew. Chem., Int. Ed. Engl.* **1999**, *38*, 1239. (d) Steiner, Th.; Saenger, W. *Acta Crystallogr.* **1992**, *B48*, 819. (e) Taylor, R.; Kennard, O.; Versichel, W. *J. Am. Chem. Soc.* **1984**, *106*, 244.

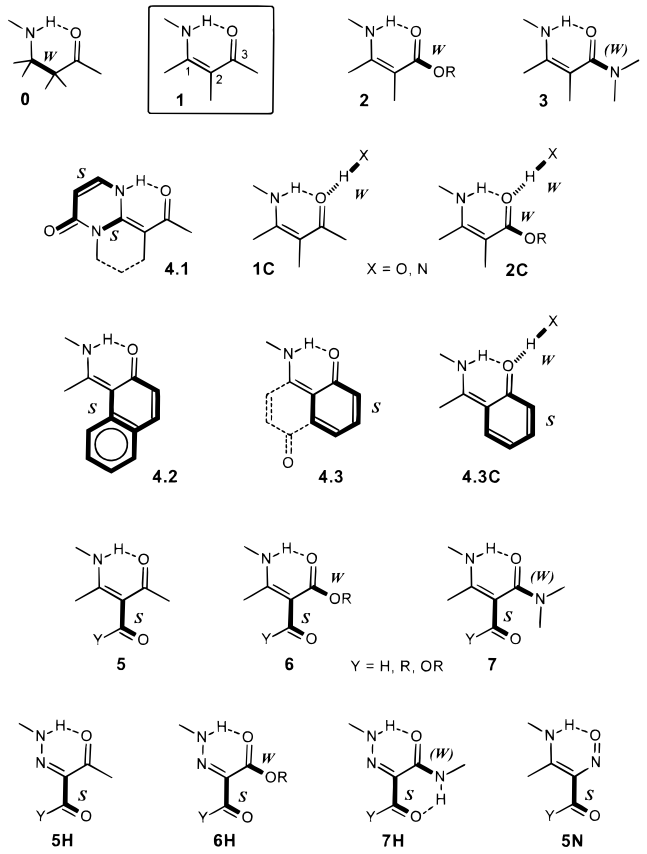

Figure 2. Chemical classes (for classification criteria, see text) in which the complete set of 133 compounds investigated has been divided according to the ability of the substituents (marked in bold) to affect the N−H···O bond with respect to simple β-enaminones **1**. The letters S and W indicate H-bond strengthening or weakening substituents, respectively.

the β-enaminonic fragment. As expected, the N···O distances are much longer in nonresonant [2.717(2) and 2.748(2) Å] than in resonant systems.

Systematic Comparison with CSD Structures. A deeper insight into the mutual relationships among π-delocalization, substituent effects, and H-bond strengthening can be achieved by a systematic CSD[12] survey (see Experimental Section) of crystal structures containing the heterodienic fragments **II**−**IV**.

The 123 compounds retrieved present a wide spectrum of different substituents, making unsuccessful any attempt of chemical classification. Therefore, an essentially pragmatic classification was adopted, simply based on the effects exerted by substituents in shortening (or lengthening) the N−H···O bond. This classification is displayed in Figure 2, where the substituents of interest are drawn in bold and are marked by the letters S and W according to whether they produce H-bond strengthening or weakening with respect to the simple enaminone **1**. Nonresonant compounds **V** are assigned to class **0**, while resonant β-enaminones **II** are divided into the following classes. **1**: simple β-enaminones; **2**: simple β-enaminoesters (3-OR-β-enaminones); **3**: simple β-enaminoamides (3-NR_2-β-enaminones); **4.1**−**4.3**: β-enaminones variously interlaced with other π-conjugated systems (class **4.1** is also 1-NR_2 substituted); **1C**, **2C**, and **4.3C**: β-enaminones of classes **1**, **2**, and **4.3** where the carbonyl is acceptor of further H-bond contacts; **5**: 2-ketoenaminones and one case of 2-(−C═C−C═O)enaminone; **6**: 2-ketoenaminoesters; and **7**: 2-ketoenaminoamides. A parallel classification has been adopted for ketohydrazones **III** and nitrosoenamines **IV** by just changing the class symbol from n to nH or nN, respectively. In practice, only examples of classes **5H**, 1,1-diketohydrazones; **6H**, 1-keto-1-esterhydrazones; **7H**, 1-keto-1-amidohydrazones; and **5N**, 2-keto-2-nitrosoenamines, were actually found in the database.

Verification of the RAHB mechanism would need to find out a correlation between N···O distances and π-delocalizations of the whole heterodienic fragment. In the present case, this was problematic because of the intrinsic dissymmetry of the heterodienic fragment and the presence of different heteroatoms and additional π-conjugated systems in many of the molecules that were studied. The problem was overcome by choosing two different indicators of π-delocalization: (i) the C═O distance in β-enaminones and ketohydrazones and, in nitrosoenamines, the N═O distance rescaled to the C═O one by subtracting 0.028 Å (the difference between N and C covalent radii); and (ii) the π-delocalization of the two HN−X═C and C−X═O moieties evaluated in terms of Pauling bond order n.[16] The π-delocalizations of the two subfragments are defined as $n_{1,2} = 1/2\ [(n_1 - 1) + (2 - n_2)]$ and $n_{3,4} = 1/2\ [(n_3 - 1) + (2 - n_4)]$, where n_1, n_2, n_3, and n_4 are the bond order of the N−X, X═C, C−X, and X═O bonds (X= C, N) having bond distances d_1, d_2, d_3, and d_4, respectively. Table 3 summarizes, for the 133 compounds investigated (123 from CSD[12] and 10 from the present paper), the average values and total ranges of N···O contact distances and C═O bond lengths, average N−H···O angles, and average delocalization indices $\langle n_{1,2}\rangle$ and $\langle n_{3,4}\rangle$. A complete list of individual values has been deposited as Tables S1−S6 of Supporting Information.

Figure 3 reports the d(C═O) vs d(N···O) scatterplots for the complete data set. The compounds have been divided into four distinct groups corresponding to the four regression lines A−D. The first group (solid symbols of Figure 3a) includes β-enaminones of classes 1−4 plus the few cases of nonresonant compounds of class 0. The related linear regression A [d(C═O) = $a + b\ d$(N···O); $a = 2.14(5)$, $b = -0.34(2)$, $r = -0.916$, and $n = 54$] confirms the interdependence between π-delocalization and H-bond shortening, supporting the effectiveness of RAHB in this system. Some β-enaminones, besides the normal intramolecular N−H···O RAHB, form further H-bonds which are accepted by the enaminonic carbonyl (classes **1C**, **2C**, and **4.3C**); their representative points (open symbols in Figure 3a) lie on another regression line, B [$a = 2.27(6)$, $b = -0.38(2)$, $r = -0.974$, and $n = 18$], which is nearly parallel and shifted upward and to the right with respect to line A, suggesting that these compounds form intramolecular RAHBs which are the same but slightly lengthened by about 0.08 Å because of the sharing of the carbonyl oxygen between two different H-bonds.[3c,15d,e] All remaining data refers to either 2-COR- or 2-COOR-substituted β-enaminones **II** (classes **5**−**7**), nitrosoenamines **IV** (class **5N**), and ketohydrazones **III** (classes **5H**−**7H**). The first four classes can be ranked together around the regression line C of Figure 3b [$a = 1.93(6)$, $b = -0.27(2)$, $r = -0.903$, and $n = 28$] that displays a slope that is somewhat lower than lines A and B, in view of a greater N···O shortening for a similar C═O delocalization. This suggests, in agreement with the results of our crystal structures, that 2-COY substitution imparts specific properties to the RAHB system which are irrespective of the nature of Y (R or OR) and are to be imputed to the very presence of the carbonyl. Similar, but less clear,

(16) (a) Pauling, L. *J. Am. Chem. Soc.* **1947**, *69*, 542. (b) Pauling, L. *The Nature of the Chemical Bond*, 3rd ed.; Cornell University Press: Ithaca, NY, 1960; p 239. (c) Pauling's bond order or, more exactly, bond number, n, is evaluated by the formula $d(n) = d(1) - c \log n$, where $d(n)$ and $d(1)$ are the bond lengths for $n = n$ and 1, respectively, and c is a constant to be evaluated for each type of chemical bond.

Table 3. Relevant Data (ranges and averages) for the 133 Compounds (123 from CSD[12] and 10 from the present structures) Forming Intramolecular N−H···O Hydrogen Bonds Arranged in Chemical Classes[a]

			d(N···O) (Å)			*d*(C=O) (Å)			
system	class	*n*	range	average	α(N−H···O) (deg)	range	average	$\langle n_{1,2}\rangle$ HN−X=C	$\langle n_{3,4}\rangle$ C−X=O
V	**0**	3	2.71−2.75	2.72[2]	144[2]	1.211−1.214	1.212[1]		
II	**1**	16	2.60−2.70	2.66[3]	139[3]	1.232−1.259	1.248[8]	0.37[7]	0.34[4]
II	**1C**	9	2.65−2.73	2.69[2]	133[4]	1.245−1.280	1.26[1]	0.45[6]	0.42[6]
II	**2**	11	2.66−2.74	2.70[2]	132[4]	1.212−1.229	1.221[6]	0.32[8]	0.19[5]
II	**2C**	3	2.73−2.76	2.75[1]	132[4]	1.230−1.240	1.234[2]	0.40[8]	0.31[9]
II	**3**	2	2.65−2.67	2.66[1]	131[5]	1.242−1.242	1.242	0.40[4]	0.19[2]
II	**4.1**	7	2.54−2.64	2.59[4]	143[3]	1.246−1.286	1.265[9]	0.39[3]	0.44[6]
II	**4.2**	10	2.51−2.57	2.54[2]	137[6]	1.277−1.309	1.289[9]	0.57[8]	0.55[7]
II	**4.3**	5	2.54−2.56	2.55[1]	143[4]	1.263−1.274	1.269[4]	0.60[9]	0.52[4]
II	**4.3C**	6	2.54−2.61	2.59[2]	144[7]	1.288−1.313	1.298[8]	0.65[7]	0.65[3]
II	**5**	19	2.52−2.64	2.56[3]	142[6]	1.236−1.266	1.250[9]	0.58[7]	0.28[4]
II	**6**	4	2.66−2.70	2.67[2]	134[2]	1.208−1.211	1.215[5]	0.37[12]	0.13[4]
II	**7**	3	2.58−2.63	2.60[2]	142[4]	1.230−1.250	1.243[9]	0.45[11]	0.20[1]
III	**5H**	14	2.56−2.63	2.58[2]	132[3]	1.219−1.237	1.228[6]	0.44[7]	0.15[3]
III	**6H**	7	2.57−2.70	2.64[4]	137[4]	1.206−1.217	1.213[3]	0.36[9]	0.11[4]
III	**7H**	12	2.54−2.61	2.58[2]	130[4]	1.221−1.248	1.232[7]	0.38[5]	0.11[3]
IV	**5N**	2	2.48−2.52	2.50[2]	143[1]	1.260−1.273	1.266[5]	0.70[1]	0.45[2]

[a] Classes: **0** = nonresonant **V**; **1**, **1C**, **2**, **2C**, and **3**−**7** = β-enaminones **II**; **5H**−**7H** = ketohydrazones **III**; and **5N** = nitrosoenamines **IV**. Individual values are available as Supporting Information Tables S1−S6. *n* = no. of structures/class. Distances, *d*, in Å and angles, α, in degrees. $\langle n_{1,2}\rangle$ and $\langle n_{3,4}\rangle$ are defined in the text.

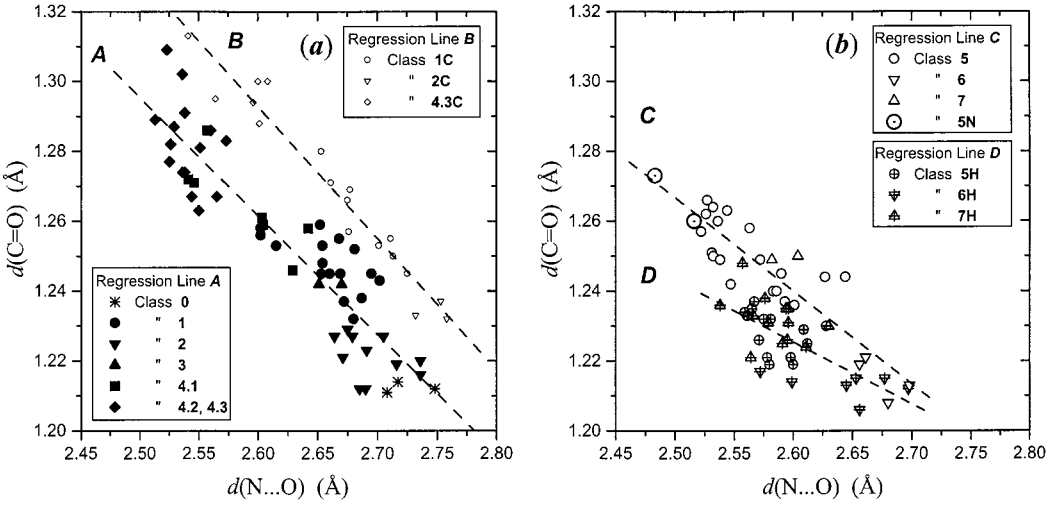

Figure 3. Scatterplots of the carbonyl bond distances, *d*(C=O) (Å), versus H-bond contact distances, *d*(N···O) (Å), for (a) β-aminones of class **0** and β-enaminones of classes **1**−**4** (regression line A) and β-enaminones of classes **1C**−**4C** (regression line B); (b) β-enaminones of classes **5**−**7** and nitrosoenamines of class **5N** (regression line C) and ketohydrazones of classes **5H**−**7H** (regression line D).

indications come from 2-COY-substituted ketohydrazones **III,** which are all grouped in a roundish cluster around the regression line D (Figure 3b) [$a = 1.69(9)$, $b = -0.18(3)$, $r = -0.688$, $n = 33$].[17]

Comparison of average N···O distances (Table 3) allows us to classify the effects exerted by substituents on H-bond strength, as schematically shown in Figure 2. Weakening substitutions turn out to be: (i) 1,2 double bond removal (cf. **0** with **1**); (ii) 3-OR (cf. **2** with **1**, **6** with **5**, and **6H** with **5H**); (iii) further H-bonds accepted by the enaminonic carbonyl (cf. **1C** with **1**, **2C** with **2**, and **4.3C** with **4.3**); (iv) possibly, 3-NR_2 (cf. **7** to **5**, though no effect is detectable by comparing **3** with **1** and **7H** with **5H**), while strengthening substitutions are (i) 1-NR_2 together with N−C=C−C=O substitution at the enaminonic nitrogen (cf. **4.1** with **1**); (ii) 2-COR and 2-COOR (cf. **5** with **1**, **6** with **2**, **7** with **3**, and the very short N···O distances in **5H** and **5N**); (iii) [2,3] fusion with a naphthalene (cf. **1** with **4.2**) or benzene ring (cf. **1** with **4.3**).

N···O distances for simple enaminones (**1**: 2.60−2.70 Å) are only slightly lengthened by the removal of the C_1=C_2 double bond (**0**: 2.71−2.75 Å), suggesting a rather weak RAHB effect in this class of heteronuclear H-bonds. The intrinsic weakness of N−H···O RAHB is correctly predicted by ECHBM, as produced by an inefficient mixing of the VB forms **IIa** and **IIb** because (i) the nitrogen PA is too high with respect to that of oxygen; and/or (ii) the ground-state energy of the VB wave function Ψ(**IIa**) is too low with respect to that of Ψ(**IIb**). These

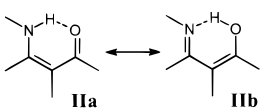

(17) The opportunity to divide all structures into the two large subsets of Figure 3a,b, respectively, is endorsed by a comparative analysis of the Pauling's π-delocalization parameters $n_{1,2}$ (HN−X=C delocalization) and $n_{3,4}$ (C−X=O delocalization; X = C, N) (Table 3) when carried out on the more symmetric 3-unsubstituted derivatives (classes **1**, **4**, **5**, **5H**, and **5N**). These molecules can now be divided into two subsets, the first for which π-delocalization is evenly distributed along the entire enaminone fragment ($\langle n_{1,2}\rangle \simeq \langle n_{3,4}\rangle$) and including all compounds of classes **1** and **4** that are not 2-COY-substituted, and the second for which $\langle n_{1,2}\rangle \gg \langle n_{3,4}\rangle$ because of the greater delocalization of the HN−X=C subfragment which was induced by 2-COY substitution (classes **5**, **5H**, and **5N**).

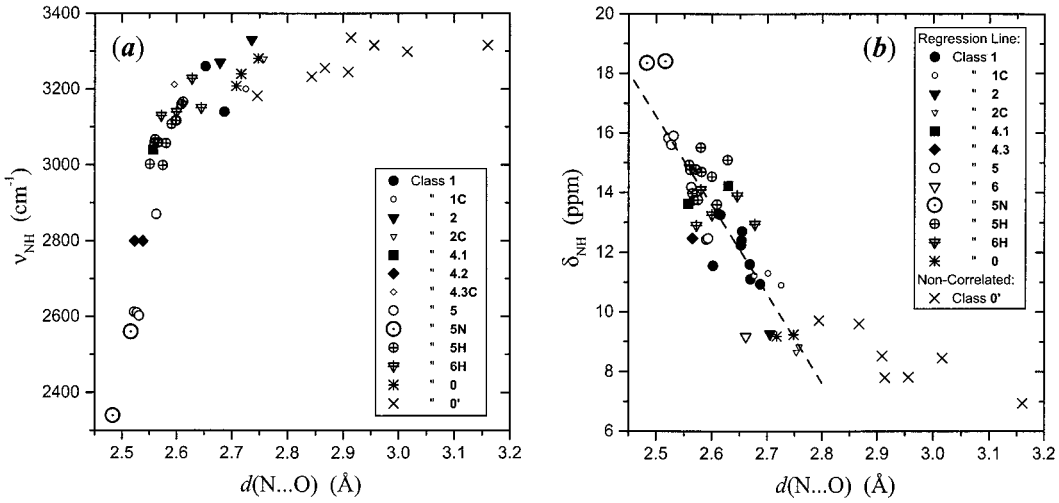

Figure 4. Scatterplots of (a) IR ν_{NH}-stretching frequencies (cm^{-1}) versus H-bond contact distances, d(N···O) (Å); (b) ^{1}H NMR δ_{NH} chemical shifts (ppm) versus H-bond contact distances, d(N···O) (Å). Crosses refer to a small set of compounds forming weak isolated H-bonds which have been reported for comparison.

rules can be reformulated in such a way as to provide a rationale for interpreting the substituent effects summarized in Figure 2.

(a) The N−H···O bond is strengthened (weakened) by electron-attracting (-donating) substituents which are able to decrease (increase) the nitrogen PA, or by electron-donating (-attracting) substituents able to increase (decrease) the oxygen PA. This can qualitatively account for the H-bond strengthening in **4.1**, **5**, **5H**, and **5N** (nitrogen charge density decreased by resonance) and again in **4.1**, as far as the 1-NR_2 group is concerned (similar decrease by induction), and for the H-bond weakening in **2** and, comparatively, in **6** and **6H** (oxygen charge density decreased by induction).

(b) The N−H···O bond is strengthened (weakened) by substituents which are able to stabilize (destabilize) Ψ(**IIb**) and/or to destabilize (stabilize) Ψ(**IIa**). This accounts for the H-bond strengthening in **4.2** in which the enamino form **IIa** is destabilized and the iminoenol tautomer **IIb** is stabilized by the loss and gain, respectively, of the resonance energy of one naphthalene ring. A similar strengthening occurs in **4.3**, although the greater resonance energy of benzene now makes the H-bonded iminoenol form ,**IIb**, more frequently observable than the enaminonic one, **IIa**.[18]

Analysis of IR and NMR Spectroscopic Data. For a number of compounds shown in Figure 3 (Tables S1−S6), it has been possible to retrieve IR-stretching frequencies, ν_{NH}, and/or ^{1}H NMR chemical shifts, δ_{NH}, of the N−H···O proton. These data are listed in Table S7 and plotted against the corresponding d(N···O) values in Figure 4. The plot of Figure 4a suggests, more than a continuous dependence of ν_{NH} on d(N···O), the presence of two different processes. In the upper part, ν_{NH} is only weakly affected by H-bond formation with a $\Delta\nu/\Delta d$ ratio of some 330 cm^{-1} Å^{-1}. This slope switches to approximately 6800 cm^{-1} Å^{-1} below a d(N···O) of 2.60 Å, around the point that marks the setting-up of the RAHB mechanism, indicating that RAHB can induce effects on the N−H bond which are more than negligible, although nondetected by X-ray diffraction (vide supra). This is confirmed by the large changes that are undergone by the IR spectrum in the ν_{NH} region because of H-bond formation, paralleling those caused by the intramolecular O−H···O bond in β-diketone enols.[4d,7d] The very narrow band of the isolated N−H is shifted from approximately 3400 cm^{-1} to lower frequencies (3300−3150 cm^{-1}), while both half-height width and integrated intensity steeply increase. Stronger H-bonds cause further red shift up to 2602 cm^{-1} for **II** (compound **c**) and 2340 cm^{-1} for **IV**,[14e] maintaining the line broadening but decreasing the intensity, which is at variance with what happens in intermolecular H-bonds, in which both widths and integrated intensities monotonically increase with the H-bond strength.[5f,g]

The effect of N···O shortening on δ_{NH} chemical shifts is shown in Figure 4b. The wide range of δ values (6.9−18.4 ppm) is a clear indication of the large deshielding of the N−H proton that may be induced by RAHB formation. The plot consists of (i) a region of approximate linearity on the left side, including resonant H-bonds, together with the two nonresonant ones, closing the same H-bonded six-membered ring **V** (compounds **f** and **g** of class **0**); and (ii) a tail in the lower right corner, including the few examples of weak intramolecular nonresonant H-bonds assumed for comparison and that do not form such a ring. The appearance of the two regions in the plot can be considered an experimental artifact due to the fact that NMR measurements are carried out in solution (usually $CDCl_3$ solutions), and chemical shifts are expected to correlate with solid-state N···O distances only for H-bonded structures (in this case, the H-bonded six-membered ring) that are stable enough to be maintained in the solution. Points belonging to the linear region have the regression equation $\delta_{NH} = 91(6) - 30(2)\,d$(N···O) ($n = 45$; $r = -0.878$), to be compared to the similar correlation [$\delta_{OH} = 100(6) - 34(3)\,d$(O···O); $n = 54$; $r = -0.88$],[19] which was obtained for the intramolecular O−H···O bond in β-diketone enols and related compounds and whose slope of 34 ppm Å^{-1} is not far from that presently observed (30 ppm Å^{-1}). This seems to indicate some parallelism between electron density movements induced by H-bond strengthening in O−H···O and N−H···O systems, despite very different lengthening of the O−H and N−H distances.

Quantum-Mechanical Calculations. The qualitative interpretation of N−H···O/ O−H···N RAHB given by ECHBM has been tested by quantum-mechanical calculations on properly

(18) A systematic CSD[12] investigation of compounds of class **4.3** shows that the large majority of them are in the iminoenolic form **IIb**, which is then to be considered the more stable for almost all combinations of substituents. The few cases of enaminone **IIa** tautomer occurrence are almost inevitably found associated with further H-bonds that are accepted by the oxygen, as sketched in **4.3C** of Figure 2, and as also noted in a recent low-temperature X-ray study by Ogawa, K.; Kasahara, Y.; Ohtani, Y.; Harada, J. *J. Am. Chem. Soc.* **1998**, *120*, 7107.

(19) Bertolasi, V.; Gilli, P.; Ferretti, V.; Gilli, G. *J. Chem. Soc., Perkin Trans. 2* **1997**, 945.

Chart 1

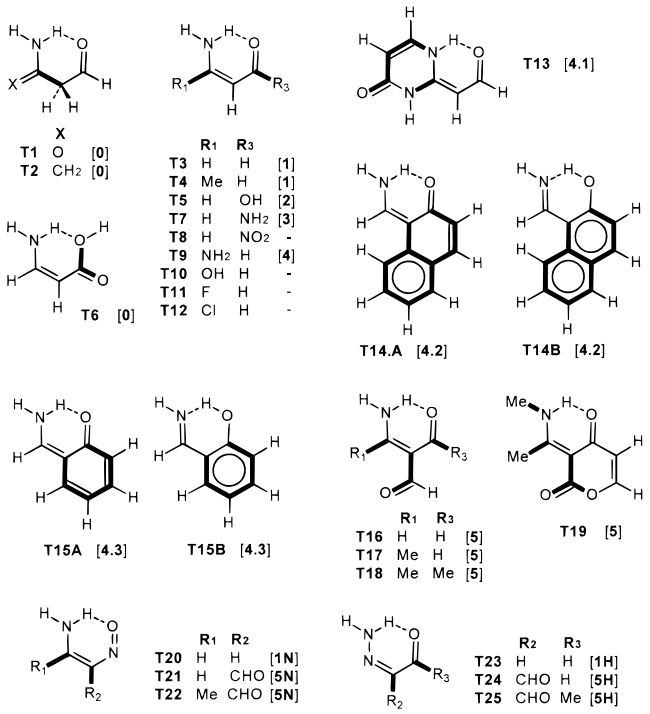

substituted sample molecules, a method which also allows one to evaluate the H-bond energies involved. Computational details are given in the Experimental Section. The 27 molecules investigated are sketched in **T1**−**T25** of Chart 1, and their relevant energetic and geometrical parameters are given in Table 4 and, in greater detail, in Table S8.

The definition itself of intramolecular H-bond energy requires some preliminary considerations. In Table 4, this energy is given as $\Delta E_{HB}(cT) = E(\text{open } cT) - E(\text{closed } cC)$, that is, the energy difference between the open (not H-bonded) *cT* and closed (H-bonded) *cC* isomers (see Table 5 for conformer definition). This quantity is hardly interpretable as a pure H-bond energy because the opening of the H-bonded form also modifies the pattern of other interatomic interactions. From this point of view, the parallel quantity $\Delta E_{HB}(cC) = E(\text{open } cC) - E(\text{closed } cC)$ seems more promising, because it represents the energy difference between two molecules without and with the H-bond, respectively, while maintaining the same interatomic repulsions, just slightly relaxed by the quantum-mechanical geometry optimization. $\Delta E_{HB}(cC)$ can be directly evaluated for the intramolecular O−H···O bond in β-diketone enols **I** removing the H-bond by a 180° rotation around the C−OH bond. Though this is made impossible in β-enaminones by the symmetry of the NH_2 group, the difference $\Delta E_{HB}(cC) - \Delta E_{HB}(cT)$ can be estimated for the parallel O−H···N bonds in **T14B** and **T15B**, which obtain values of 4.27 and 4.34 kcal mol^{-1}, respectively. At a first approximation, it can then be assumed that $\Delta E_{HB}(cC)$ is greater than $\Delta E_{HB}(cT)$ by approximately 4.30 kcal mol^{-1} for all N−H···O/O−H···N bonds shown in Table 4, whose energies can now be more easily compared to those of β-diketone enols **I**. For reference, $\Delta E_{HB}(cC)$, $\Delta E_{HB}(tC)$, and $\Delta E_{HB}(cT)$ are calculated, at the same B3LYP/6-31+G(d,p) level without ZPC, to be 13.56, 10.56, and 9.51 for malondialdehyde, and 16.39, 14.20, and 13.08 kcal mol^{-1} for acetylacetone, values that, when lowered by 0.5−1.0 kcal mol^{-1} to account for ZPC, compare well to others previously reported ($\Delta E_{HB}(cC) = 12.4$ and 13.3 for malondialdehyde[20a,c] and $\Delta E_{HB}(tC) = 12.0$ kcal mol^{-1} for acetylacetone[20b]). Notice, however, that the evaluation of intramolecular H-bond energies may be made complicated, and sometimes impossible, by the presence of substituents that cause all open forms to have strong attractive or repulsive nonbonded interactions. In these difficult cases, H-bond energies lose their meaning and cannot be calculated (compounds **T19**, **T21**, **T22**, **T24**, and **T25**).

The optimized H-bond geometries shown in Table 4 are in reasonable agreement with the average experimental values of Table 3, confirming the validity of the computational model chosen. The agreement with the experiments is corroborated by the comparison of the interatomic distances for the crystal structure of compound **d** and its simulated counterpart **T19**, which are d(N···O) = 2.563 and 2.560, d(C═O) = 1.258 and 1.258, d(C−C) = 1.445 and 1.461, d(C═C) = 1.438 and 1.429, and d(C−N) = 1.303 and 1.330 Å, respectively. In the following discussion, $\Delta E_{HB}(cT)$ (kcal mol^{-1}) and d(N···O) (Å) values for each optimized sample molecule will be indicated by two figures enclosed in square brackets, that is, [$\Delta E_{HB}(cT)$; d(N···O)].

The three reference molecules for β-enaminones **II**, ketohydrazones **III**, and nitrosoenamines **IV** are **T3** [5.22; 2.713], **T23** [7.03; 2.676], and **T20** [6.12; 2.615], respectively. Their H-bond energies fall in the restricted range of 5.2−7.0 kcal mol^{-1}, confirming that heteronuclear N−H···O RAHBs are systematically weaker than the homonuclear O−H···O ones (e.g., $\Delta E_{HB}(cT) = 9.51$ and 13.08 kcal mol^{-1} in malondialdehyde and acetylacetone, respectively). The contribution of resonance to the H-bond energy is not irrelevant, however, as shown by the comparison of the simple β-enaminone **T3** [5.22; 2.713] to **T1** [2.78; 2.788] and **T2** [2.72; 2.794], two molecules in which the π-conjugated system is interrupted by C═C double bond removal.

Crystal structures (see Figure 2) indicate a sensible H-bond weakening due to 3-OR and a smaller one due to 3-NR_2 substitution. These effects are confirmed by calculations as shown by the comparison of the reference β-enaminone **T3** [5.22; 2.713] to its 3-OH **T5** [4.00; 2.749] and 3-NH_2 **T7** [4.74; 2.719] derivatives. In the β-enaminoester, **T5**, the RAHB has become so weak that it is barely distinguishable from its nonresonant isomer, **T6** [3.25; 2.741]. The negative influence of electron-attracting 3-substitution is also shown by the 3-NO_2-enaminone **T8** [3.61; 2.757], for which no experimental data are, however, available.

According to **4.1** (Figure 2), the 1-NR_2 and/or the *N*−C═C−C═O substituents are to be classified as electron-attracting H-bond strengthening groups. This is verified by calculations for the 1-NH_2-enaminone **T9** [7.06; 2.661] and for compound **T13** [9.11; 2.622] in which both substituents are present. The strengthening effects of substituents that are able to increase N−H acidity by withdrawing electrons from the nitrogen are confirmed by **T10** [9.52; 2.649], **T11** [8.04; 2.690], and **T12** [8.01; 2.677] carrying the 1-OH, 1-F and 1-Cl substituents, respectively, but for which no crystal structures are available for comparison.

The effect of 2-CHO substitution in **II**, **III** and **IV** is illustrated by the pairs {**T3** [5.22; 2.713]; **T16** [6.66; 2.701]}, {**T23** [7.03; 2.676]; **T24** [−; 2.651]}, and {**T20** [6.12; 2.615]; **T21** [−; 2.614]}, respectively. This substituent was classified as H-bond strengthening in Figure 2, but calculations indicate that it produces, per se, a weak $\Delta E_{HB}(cT)$ increase, when

(20) (a) Frisch, M. J.; Scheiner, A. C.; Schaefer, H. F., III; Binkley, J. S. *J. Chem. Phys.* **1985**, *82*, 4194. (b) Dannenberg, J. J.; Rios, R. *J. Phys. Chem.* **1994**, *98*, 6714. (c) Buemi, G.; Zuccarello, F. *J. Chem. Soc., Faraday Trans.* **1996**, *92*, 347. (d) Buemi, G.; Zuccarello, F. *Electron. J. Theor. Chem.* **1997**, *2*, 118. (e) Filarowski, A.; Głowiak, T.; Koll, A. *J. Mol. Struct.* **1999**, *484*, 75.

Table 4. DFT Optimized Bond Distances and Angles (Å and deg) and H-Bond Energies $\Delta E_{HB}(cT)$ (kcal mol^{-1}) for Intramolecularly H-Bonded β-Enaminones (**T3**−**T19**), Ketohydrazones (**T23**−**T25**), Nitrosoenamines (**T20**−**T22**), and β-Ketoaminones (**T1**, **T2**, and **T6**)[a]

no.	$\Delta E_{HB}(cT)$[b]	N···O	N−H N··H	H··O H−O	N−H−O	C═O C−O d_1	C−C C═C d_2	C═C C−C d_3	C−N C═N d_4	$\langle\Delta d\rangle$	class
T1	2.78[c]	2.788	1.013	2.008	131.9	1.217	1.509	1.535	1.355	8.5	**0**
T2	2.72[d]	2.794	1.012	2.012	132.5	1.217	1.508	1.524	1.375	7.5	**0**
T3	5.22	2.713	1.019	1.956	128.8	1.243	1.437	1.376	1.345	13.8	**1**
T4	6.24	2.684	1.022	1.891	131.9	1.246	1.431	1.385	1.347	12.3	**1**
T5	4.00	2.749	1.016	2.021	126.5	1.236	1.442	1.369	1.349	10.8	**2**
T6	3.25	2.741	1.010	2.070	121.8	1.221	1.449	1.365	1.354	9.0	**0**
T7	4.74	2.719	1.017	1.974	127.9	1.247	1.458	1.367	1.351	12.3	**3**
T8	3.61	2.757	1.016	2.032	126.2	1.214	1.420	1.380	1.340	10.3	
T9	7.06[e]	2.661	1.027	1.828	135.7	1.252	1.420	1.399	1.349	16.5	**4.1**
T10	9.52[c]	2.649	1.029	1.820	135.0	1.250	1.426	1.384	1.346	20.1	
T11	8.04[c]	2.690	1.023	1.916	130.0	1.244	1.435	1.371	1.334	16.8	
T12	8.01[c]	2.677	1.025	1.878	132.3	1.243	1.438	1.375	1.339	16.5	
T13	9.11[e]	2.622	1.037	1.753	138.6	1.252	1.426	1.389	1.368	16.5	**4.1**
T14A	8.61[f]	2.571	1.031	1.750	133.5	1.261	1.466	1.392	1.334	20.5	**4.2**
T14B	11.34	2.541	1.630	1.011	147.5	1.336	1.412	1.451	1.295	20.3	**4.2**
T15A	9.45	2.581	1.038	1.730	136.2	1.266	1.469	1.397	1.329	19.0	**4.3**
T15B	9.99	2.614	1.721	0.998	146.8	1.343	1.423	1.454	1.290	18.0	**4.3**
T16	6.66[e]	2.701	1.022	1.936	129.2	1.239	1.444	1.392	1.328	14.5	**5**
T17	8.67[e]	2.632	1.027	1.808	134.6	1.242	1.444	1.414	1.332	18.3	**5**
T18	8.82[e]	2.571	1.028	1.743	134.6	1.248	1.465	1.418	1.333	18.8	**5**
T19		2.560	1.039	1.650	143.3	1.258	1.461	1.429	1.330		**5**

no.	$\Delta E_{HB}(cT)$	N···O	N−H	H··O	N−H−O	N═O d_1	N−C d_2	C═C d_3	C−N d_4	$\langle\Delta d\rangle$	class
T20	6.12	2.615	1.022	1.868	127.2	1.262	1.372	1.386	1.335	20.5	**1N**
T21		2.614	1.021	1.884	125.6	1.250	1.393	1.394	1.328		**5N**
T22		2.542	1.031	1.727	132.8	1.256	1.384	1.417	1.329		**5N**

no.	$\Delta E_{HB}(cT)$	N···O	N−H	H··O	N−H−O	C═O d_1	C−C d_2	C═N d_3	N−N d_4	$\langle\Delta d\rangle$	class
T23	7.03	2.676	1.021	1.915	128.7	1.238	1.449	1.313	1.313	17.3	**1H**
T24		2.651	1.024	1.883	129.2	1.234	1.464	1.323	1.301		**5H**
T25		2.589	1.024	1.820	128.9	1.240	1.485	1.325	1.300		**5H**

[a] ΔE_{HB} values were obtained by comparing the H-bonded (closed) and non-H-bonded (open) forms, whose geometries and energies are listed in Table S8. Calculations at the B3LYP/6-31+G(d,p)//B3LYP/6-31+G(d,p) level of theory without ZP correction. $\langle\Delta d\rangle$ is a measure of the increased delocalization of the π-conjugated system which is induced by H-bond formation and is defined as $\langle\Delta d\rangle = \langle(-1)^i[d_i(\text{non-H-bonded}) - d_i(\text{H-bonded})]\rangle_i \cdot 1000$. Class is the chemical class defined in Figure 2 and Table 3. [b] H-bond energies, $\Delta E_{HB}(cT)$, refers to the open *cT* isomer of C_s symmetry except when specifically indicated in *c*−*f*. ΔE_{HB} values are missing for compounds for which *all* open conformations display unwanted interatomic attractions or repulsions: [c]ΔE_{HB} refers to the *tt* open isomer without corrections, [d]ΔE_{HB} refers to the average of the three possible open isomers, [e]ΔE_{HB} refers to the open *tC* isomer and is renormalized to $\Delta E_{HB}(cT)$ by subtracting 2.38 kcal mol^{-1} = $\Delta E_{HB}(tC) - \Delta E_{HB}(cT)$ (see Table 5), [f]*cT* open form optimized in the C_1 point group.

Table 5. DFT and MP2 ab Initio Optimized Geometries (Å and deg), H-Bond Energies ΔE_{HB} (kcal mol^{-1}), and Vibration Frequencies (cm^{-1}) for the β-Enaminone Molecule in Its H-Bonded (closed) and Not H-Bonded (open) Planar Conformations[a]

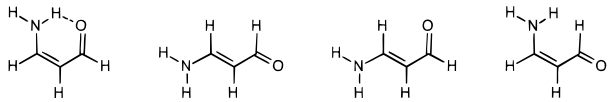

	method	ΔE_{HB}	ΔE_{HB}^{ZPC}	ΔG_{HB}	N···O	N−H	H···O	N−H−O	C═O d_1	C−C d_2	C═C d_3	C−N d_4	$\langle\Delta d\rangle$	$\nu_a(NH_2)$	$\nu_s(NH_2)$	ν(C═O)
cC	B3LYP	0.0	0.0	0.0	2.713	1.019	1.956	128.8	1.243	1.437	1.376	1.345	0.0	3718	3472	1709
	MP2	0.0			2.702	1.015	1.951	128.5	1.252	1.437	1.373	1.347	0.0			
tT	B3LYP	4.43	3.55	2.54		1.007			1.226	1.448	1.360	1.358	14.2	3753 (35)	3624 (152)	1745 (36)
	MP2	4.53				1.005			1.236	1.448	1.359	1.361	13.8			
cT	B3LYP	5.22	4.54	3.97		1.007			1.230	1.454	1.362	1.356	13.8	3748 (30)	3618 (146)	1750 (41)
	MP2	5.48				1.005			1.239	1.455	1.360	1.358	13.8			
tC	B3LYP	7.60	6.65	6.39		1.006			1.227	1.447	1.365	1.362	13.5	3759 (41)	3633 (161)	1737 (28)
	MP2	7.63				1.004			1.238	1.447	1.364	1.365	12.8			

[a] DFT calculations at the B3LYP/6-31+G(d,p)//B3LYP/6-31+G(d,p) level and ab initio calculations at the MP2/6-31+G(d,p)//MP2/6-31+G(d,p) level of theory. ZP corrections and vibrational frequencies have been evaluated only for the B3LYP case. ΔE_{HB}^{ZPC} and ΔG_{HB} are the H-bond zero-point corrected and Gibbs free energies (kcal mol^{-1}). $\langle\Delta d\rangle$ is a measure of the increased delocalization of the π-conjugated system induced by H-bond formation and is defined as $\langle\Delta d\rangle = \langle(-1)^i[d_i \text{ (non-H-bonded)} - d_i \text{ (H-bonded)}]\rangle_i \cdot 1000$. Figures in parentheses are differences between frequencies of H-bonded and non-H-bonded forms.

available, and a weak N···O contraction. Its strengthening role becomes more evident in association with other bulky substituents (see **T17** and **T18** below) and can be imputed, besides steric factors, to an increase of both N−H acidity and C═O basicity. This change of acid−base properties is consistent with the parallel changes in bond distances which are produced by 2-CHO-substitution within the O═C−C═C−NH fragment (Tables 4 and S8) and which indicate a large increase in the

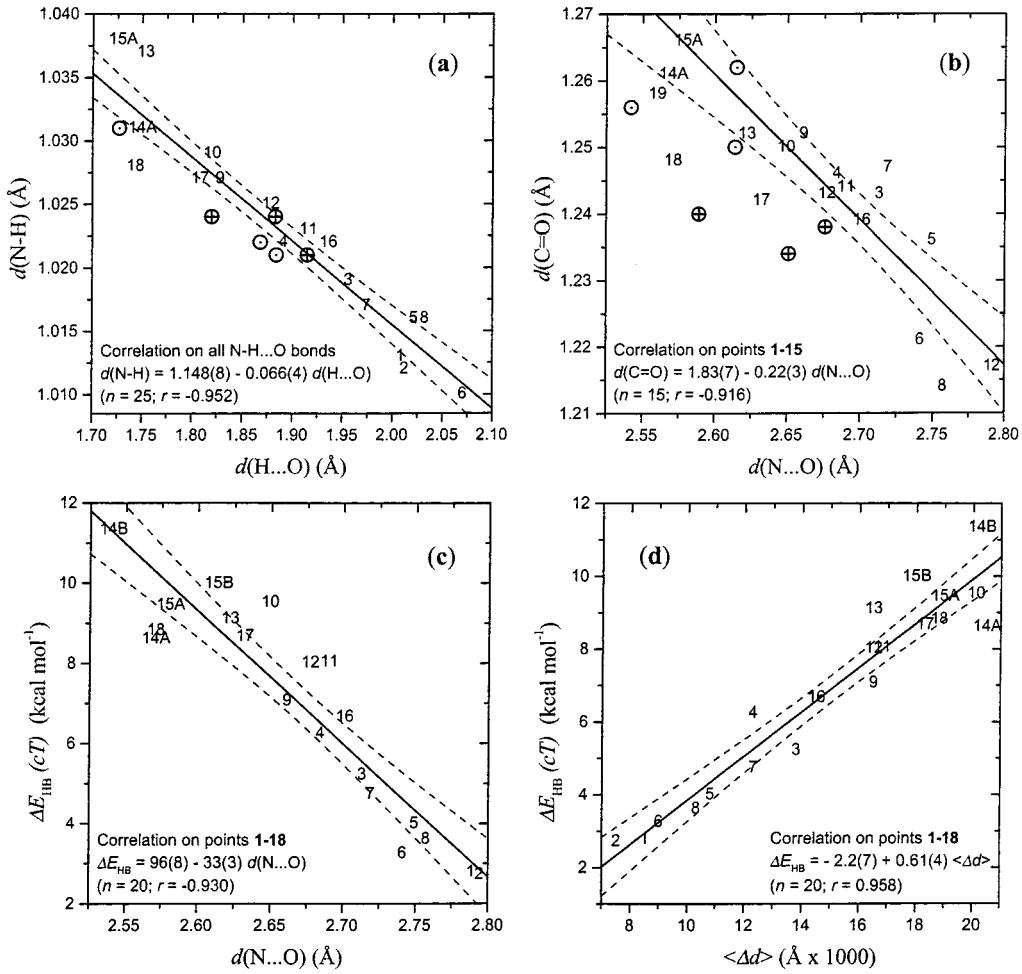

Figure 5. Correlation diagrams among geometric and energy parameters which are obtained from the quantum-mechanical optimization of sample molecules **T1**−**T25** (Chart 1 and Table 4). Distances in Å and H-bond energies, $\Delta E_{HB}(cT)$, in kcal mol^{-1}. Figures refer to enaminones, crossed and dotted circles to ketohydrazones and nitrosoenamines, respectively. Dashed lines around the continuous linear regression lines are confidence limits at 95% probability.

C═C−NH and a parallel, though smaller, decrease of the O═C−C π-delocalizations ($n_{1,2}$ = 0.370, 0.486, 0.540, and 0.549; $n_{3,4}$ = 0.282, 0.250, 0.260, and 0.221 for **T3**, **T16**, **T17**, and **T18**, respectively).

The six-membered ring of R_3−RAHB is a rather crowded structure in which further substituents can induce H-bond strengthening by mutual repulsion.[3b,20e] This is verified by the comparison of the simple β-enaminone **T3** [5.22; 2.713] to its 1-Me derivative **T4** [6.24; 2.684], and of the 2-CHO-enaminone **T16** [6.66; 2.701] to its 1-Me and 1,3-diMe derivatives, **T17** [8.67; 2.632] and **T18** [8.82; 2.571], respectively. These last optimizations seem to suggest that, beyond a certain limit, the increasing steric strain may shorten the H-bond without increasing its energy, possibly because of internal compensation between the parallel increase of H-bond and repulsion forces.

Of particular interest are molecules **T14** and **T15**, which can form either N−H···O or O−H···N bonds because of the competition between the energy gain due to RAHB and the loss of resonance energy of the naphthalene or benzene ring (approximately 25 and 36 kcal mol^{-1}, according to thermochemical measurements[21]). In β-enaminonic systems, the N−H···O bond is by far more stable than the O−H···N one. For reference, the N−H···O-bonded simple β-enaminone **T3** is 8.00 kcal mol^{-1} lower in total energy than its O−H···N-bonded enolimine tautomer (not listed in Table 4). This energy difference is heavily perturbed by condensation with aromatic moieties. It is almost completely lost because of fusion with the naphthalene ring, and the N−H···O-bonded β-enaminone **T14A** [8.61; 2.571] is still slightly more stable, by 0.45 kcal mol^{-1}, than the O−H···N-bonded enolimine **T14B** [11.34; 2.541]. The proton position is, finally, reversed by the greater benzene resonance energy, and the N−H···O-bonded β-enaminone **T15A** [9.45; 2.581] has been calculated to be 3.57 kcal mol^{-1} higher in energy than the enolimine **T15B** [9.99; 2.614], which has now become, in agreement with crystal structural evidence,[18] the more stable form of the H-bonded molecule.

Figure 5 reports some correlations between calculated parameters for the molecules of Table 4 and Chart 1. Statistical correlations have been confined to β-enaminones **II** data (**T1**−**T19**) because of several systematic differences displayed by ketohydrazones **III** (**T23**−**T25**) and nitrosoenamines **IV** (**T20**−**T22**). The only exception is represented by the d(N−H) vs d(H···O) scatterplot (Figure 5a), in which the three classes can be joined together around the same regression line (r = −0.962 for **II** only, and r = −0.952 for **II**, **III**, and **IV**), displaying the same common behavior as in the IR ν_{NH} vs d(N···O) and ^{1}H NMR δ_{NH} vs d(N···O) scatterplots of Figure 4, and supporting the idea of a unique law of N−H vs H···O interdependence in the N−H···O moiety of the three classes of compounds. Calculated d(N−H) values agree with crystal data (vide supra)

(21) March, J. *Advanced Organic Chemistry*, 3rd ed.; John Wiley & Sons: New York, 1985; p 40.

in confirming the very small lengthening of the N−H bond that is produced by H-bond formation. Even in the most elongated N−H bonds [d(N−H) = 1.039, 1.038, and 1.037 Å in **T19**, **T15A**, and **T13**, respectively] the N−H lengthening is smaller than 0.03 Å with respect to the unperturbed N−H distance of approximately 1.011 Å,[14a,d] so that the N−H···O bond remains strongly dissymmetric. The rather large H-bond-induced changes of IR ν_{NH} (from ≃3400 to 2300−2400 cm^{-1}) and of ^{1}H NMR δ_{NH} (from ≃7 to 16−18 ppm) are then to be imputed to RAHB-induced electron shifts within the conjugated heterodiene more than to a displacement of the proton within the N−H···O moiety.

The plot of Figure 5b shows the usual correlation between H-bond strengthening and C═O lengthening which agree, at least qualitatively, with Figure 3 in indicating that ketohydrazones **III** (crossed circles) and 2-CHO-substituted derivatives (**T16**−**T18**) have smaller C═O lengthenings for the same N···O shortening than do β-enaminones **II** (**T1**−**T15**). The slope of the regression that includes β-aminones and β-enaminones which are not 2-CHO-substituted (**T1**−**T15**) is, however, only −0.22, that is, somewhat smaller than the experimental one (−0.34: regression A of Figure 3). This discrepancy seems to be imputable to the presence of many other substituents in the real molecules that cannot be accounted for in the simplified sample molecules.

Of particular interest is the overall pattern of ΔE_{HB} changes due to chemical substituents (Figure 5c). The value obtained for the simple β-enaminone **T3** ($\Delta E_{HB}(cT)$ = 5.22 kcal mol^{-1}) is rather small, in agreement with ECHBM predictions on heteronuclear RAHBs, but can be easily modulated by proper substitutions at the enaminone fragment **II** to give H-bond energies approximately two times as large. For all sample molecules investigated, calculated ΔE_{HB} values are in good qualitative agreement with ECHBM expectations and rather strictly correlated with the N···O contact distance (Figure 5c) and the degree of π-delocalization of the enaminone fragment Δd (Figure 5d), showing that, despite the variety of chemical substitutions, the ultima ratio of H-bond strengthening relies on the RAHB mechanism.

Conclusions

This work was designed to show that two concepts originally developed for the homonuclear H-bond, that is, RAHB (resonance-assisted H-bond)[3b,c] and ECHBM (electrostatic-covalent H-bond model),[3a] can be applied as well to the heteronuclear N−H···O bond and, in particular, to the intramolecular N−H···O R_3−RAHB occurring in β-enaminones (and other related heterodienes).

The role played by resonance, that is, the effectiveness of RAHB in strengthening the intramolecular H-bond in β-enaminones, is widely confirmed by the comparison of H-bonded β-enaminone **II** and β-aminone **V** geometries either obtained by X-ray crystallography for this paper (Table 2) or derived from structural databases (Table 3) or simulated by quantum-mechanical optimization carried out by rather advanced DFT methods (Table 4).

The H-bond energy for the reference β-enaminonic molecule, the simple β-enaminone **T3**, is rather small ($\Delta E_{HB}(cT)$ = 5.22 kcal mol^{-1}) when compared to those calculated at the same level of theory for the intramolecular O−H···O bond in malondialdehyde ($\Delta E_{HB}(cT)$ = 9.51 kcal mol^{-1}) and acetylacetone ($\Delta E_{HB}(cT)$ = 13.08 kcal mol^{-1}), which are not among the shortest H-bonds in the class of intramolecularly H-bonded β-diketone enols, confirming the ECHBM prediction that N−H···O heteronuclear bonds are intrinsically weaker because of the PA difference between H-bond donor and acceptor atoms. Comparison between resonant (**T3**) and nonresonant (**T1** and **T2**) forms suggests that the contribution of resonance to ΔE_{HB} amounts to approximately 2.5 over 5.22 kcal mol^{-1}, which compares well with the parallel estimate for acetylacetone,[20b] which amounts to 6.0 over 12.0 kcal mol^{-1}.

Though intrinsically weaker than in the homonuclear case, the H-bond in β-enaminones benefits from the interesting property that it can be shortened, and its energy enhanced, by proper substituents able to reduce the PA gap between the H-bond donor and the acceptor atom and/or the energy gap between the enamino (**IIa**) and iminoenol (**IIb**) tautomeric forms. This property is correctly predicted by ECHBM, empirically verified by a large number of crystal structures, and definitely confirmed by quantum-mechanical DFT calculations. H-bond energies can be nearly doubled by substitution, thus making the strength of the heteronuclear N−H···O RAHB comparable with that of its homonuclear O−H···O counterpart.

A final argument in favor of the importance of N−H···O RAHB comes from the fact that other R_3-heteroconjugated fragments, such as ketohydrazones **III** and nitrosoenamines **IV**, form intramolecular H-bonds that strictly reproduce the behavior (resonance-induced H-bond shortening, effect of substituents, N···O dependence of the IR ν_{NH} stretching frequencies, and ^{1}H NMR δ_{NH} chemical shifts) of β-enaminones **II**, clearly indicating that, as far as the H-bond formation is concerned, the stereoelectronic similarities (identical π-conjugation scheme) are more important than the chemical diversities.

Experimental Section

Crystal Structure Analysis. Compounds **a**−**d** were synthesized[22a] by Schiff-base condensation of dehydroacetic acid with a suitable amine. Compound **e** was obtained[22b,c] by nitrosation of *p*-methoxyphenylamino-5,5-dimethyl-2-cyclohexen-1-one. Compounds **f** and **g** were purchased from Aldrich. X-ray diffraction data for compounds **a**−**g** were collected at room temperature on an Enraf-Nonius CAD4 diffractometer with graphite-monochromated Mo Kα radiation (λ = 0.71069 Å) and $\omega/2\theta$ scan technique ($2 \le \theta \le 28°$). Lattice constants were determined by least-squares fitting of the setting angles of 25 reflections in the range $10 \le \theta \le 14°$. Intensities of three standard reflections were measured every 2 h and did not show significant variations for any of the compounds investigated. Scattering factors were taken from ref 23a. All structures were solved by direct methods with the SIR92 package[23b] and refined by full-matrix least-squares with anisotropic non-H and isotropic H atoms. An attempt was made to refine the enamino H atom anisotropically. The refinement succeeded for compunds **a**, **b**, and **d**. The size and shape of the final proton thermal ellipsoids (Figure 1) are rather similar among themselves and not dissimilar to those found in 1,3-diaryl-1,3-propanedione enols.[3c,24] Calculations were accomplished by the MolEN package[23c] and PARST.[23d,e] X-ray diffraction data for compounds **a**, **b**, and **c** (hereafter indicated as **a′**, **b′**, and **c′**) were independently collected at 150 K on a Philips PW1100 diffractometer

(22) (a) Liu, S.; Rettig, S. J.; Orvig, C. *Inorg. Chem.* **1991**, *30*, 4915. (b) Cromwell, N. H.; Miller, F. A.; Johnson, A. R.; Frank, R. L.; Wallace, D. L. *J. Am. Chem. Soc.* **1949**, *71*, 3337. (c) Bertolasi, V.; Gilli, P.; Ferretti, V.; Gilli, G. *Acta Crystallogr.* **1998**, *B54*, 50.

(23) (a) Cromer, D. T.; Waber, J. T. *International Tables for X-ray Crystallography*; Kynoch Press (present distributor, Kluwer Academic Publishers: Dordrecht): Birmingham, U.K., 1974; Vol. IV, p 149. (b) Altomare, A.; Cascarano, G.; Giacovazzo, C.; Guagliardi, A.; Burla, M. C.; Polidori, G.; Camalli, M. *J. Appl. Crystallogr.* **1994**, *27*, 435. (c) Fair, C. K. *MolEN. An Interactive Intelligent System for Crystal Structure Analysis*; Enraf-Nonius: Delft, The Netherlands, 1990. (d) Nardelli, M. *Comput. Chem.* **1983**, *7*, 95. (e) Nardelli, M. *J. Appl. Crystallogr.* **1995**, *28*, 659. (f) Hall, S. R.; Flack, H. D.; Stewart, J. M. *XTAL3.2*; University of Western Australia, Lamb: Perth, 1994. (g) Sheldrick, G. M. *SHELXL93. Program for Refinement of Crystal Structures*; University of Gottingen: Germany, 1993.

(24) Jones, R. D. G. *Acta Crystallogr.* **1976**, *B32*, 187.

with graphite monochromated Cu Kα radiation ($\lambda = 1.54180$ Å) and $\omega/2\theta$ scan technique ($4 \le \theta \le 65°$). Lattice constants were determined by least-squares fitting of the setting angles of 60 reflections in the range $6 \le \theta \le 45°$, and the intensities of 2 standard reflections measured every 1.5 h did not show significant variations for any of the compounds investigated. All structures were refined by full-matrix least-squares with anisotropic non-H and isotropic H atoms. The enamino hydrogens of compounds **a′** and **b′** were refined anisotropically. The thermal ellipsoid orientations are very similar to those determined at room temperature, while their size is, of course, somewhat smaller. Calculations were accomplished by XTAL3.2,[23f] SHELX-93,[23g] and PARST.[23d,e]

Crystal data for a: 3-(1-phenylaminoethylidene)-6-methyl-3*H*-pyran-2,4-dione, $C_{14}H_{13}NO_3$, $M_r = 243.26$, monoclinic $P2_1/c$ (no. 14), colorless, $a = 11.881(1)$, $b = 7.921(1)$, $c = 12.893(7)$ Å, $\beta = 91.10(3)°$, $V = 1213.1(7)$ Å^3, $Z = 4$, $D_{calc} = 1.33$ g cm^{-3}, $\mu = 0.94$ cm^{-1}, and $T = 295$ K. Of the 3516 unique measured reflections, 2145 with $I > 3\sigma(I)$ were used in the refinement. R(on F) = 0.044, $R_w = 0.060$, and $S = 2.02$.

Crystal data for a′: 3-(1-phenylaminoethylidene)-6-methyl-3*H*-pyran-2,4-dione, $C_{14}H_{13}NO_3$, $M_r = 243.26$, monoclinic $P2_1/c$ (no. 14), colorless, $a = 11.820(1)$, $b = 7.713(1)$, $c = 12.974(1)$ Å, $\beta = 91.12(1)°$, $V = 1182.6(2)$ Å^3, $Z = 4$, $D_{calc} = 1.37$ g cm^{-3}, $\mu = 7.96$ cm^{-1}, and $T = 150$ K. Of the 2010 unique measured reflections, 1966 with $I > 2\sigma(I)$ were used in the refinement. R(on F^2) = 0.040, $R_w = 0.102$, and $S = 1.17$.

Crystal data for b: 3-[1-(4-methoxyphenylamino)ethylidene]-6-methyl-3*H*-pyran-2,4-dione, $C_{15}H_{15}NO_4$, $M_r = 273.28$, monoclinic $P2_1/a$ (no. 14), pale yellow, $a = 12.982(2)$, $b = 7.680(2)$, $c = 14.015(1)$ Å, $\beta = 107.53(5)°$, $V = 1332.4(6)$ Å^3, $Z = 4$, $D_{calc} = 1.36$ g cm^{-3}, $\mu = 0.99$ cm^{-1}, and $T = 295$ K. Of the 3880 unique measured reflections, 2043 with $I > 3\sigma(I)$ were used in the refinement. R(on F) = 0.046, $R_w = 0.057$, and $S = 1.79$.

Crystal data for b′: 3-[1-(4-methoxyphenylamino)ethylidene]-6-methyl-3*H*-pyran-2,4-dione, $C_{15}H_{15}NO_4$, $M_r = 273.28$, monoclinic $P2_1/a$ (no. 14), pale yellow, $a = 12.999(2)$, $b = 7.547(1)$, $c = 13.974(2)$ Å, $\beta = 107.69(1)°$, $V = 1306.1(3)$ Å^3, $Z = 4$, $D_{calc} = 1.39$ g cm^{-3}, $\mu = 8.41$ cm^{-1}, and $T = 150$ K. Of the 2222 unique measured reflections, 2108 with $I > 2\sigma(I)$ were used in the refinement. R(on F^2) = 0.044, $R_w = 0.122$, and $S = 1.12$.

Crystal data for c: **3**-[1-(4-chlorophenylamino)ethylidene]-6-methyl-3*H*-pyran-2,4-dione, $C_{14}H_{12}ClNO_3$, $M_r = 277.71$, triclinic $P\bar{1}$ (no. 2), colorless, $a = 7.401(1)$, $b = 8.364(2)$, $c = 10.683(2)$ Å, $\alpha = 97.51(1)$, $\beta = 103.45(1)$, $\gamma = 92.69(1)°$, $V = 635.6(2)$ Å^3, $Z = 2$, $D_{calc} = 1.45$ g cm^{-3}, $\mu = 3.03$ cm^{-1}, and $T = 295$ K. Of the 3698 unique measured reflections, 2473 with $I > 2\sigma(I)$ were used in the refinement. R(on F) = 0.043, $R_w = 0.062$, and $S = 2.14$.

Crystal data for c′: 3-[1-(4-chlorophenylamino)ethylidene]-6-methyl-3*H*-pyran-2,4-dione, $C_{14}H_{12}ClNO_3$, $M_r = 277.71$, triclinic $P\bar{1}$ (no. 2), colorless, $a = 7.3373(5)$, $b = 8.2919(5)$, $c = 10.590(9)$ Å, $\alpha = 98.525(9)$, $\beta = 102.805(5)$, $\gamma = 91.989(7)°$, $V = 619.8(5)$ Å^3, $Z = 2$, $D_{calc} = 1.49$ g cm^{-3}, $\mu = 27.72$ cm^{-1}, and $T = 150$ K. Of the 2118 unique measured reflections, 2110 with $I > 2\sigma(I)$ were used in the refinement. R(on F^2) = 0.036, $R_w = 0.107$, and $S = 1.16$.

Crystal data for d: *N,N′*-3-azapentane-1,5-bis[3-(1-aminoethylidene)-6-methyl-3*H*-pyran-2,4-dione], $C_{20}H_{25}N_3O_6$, $M_r = 403.43$, monoclinic $C2/c$ (no. 15), colorless, $a = 13.210(4)$, $b = 14.666(2)$, $c = 10.130(3)$ Å, $\beta = 92.46(2)°$, $V = 1960.8(9)$ Å^3, $Z = 4$, $D_{calc} = 1.37$ g cm^{-3}, $\mu = 1.02$ cm^{-1}, and $T = 295$ K. Of the 2857 unique measured reflections, 1855 with $I > 3\sigma(I)$ were used in the refinement. R(on F) = 0.046, $R_w = 0.059$, and $S = 1.96$.

Crystal data for e: 3-(3-methoxyphenylamino)-5,5-dimethyl-2-nitroso-2-cyclohexen-1-one, $C_{15}H_{18}N_2O_3$, $M_r = 274.32$, triclinic $P\bar{1}$ (no. 2), intense blue, $a = 8.934(2)$, $b = 10.930(1)$, $c = 8.044(3)$ Å, $\alpha = 106.24(2)$, $\beta = 114.49(2)$, $\gamma = 83.28(1)°$, $V = 686.3(3)$ Å^3, $Z = 2$, $D_{calc} = 1.33$ g cm^{-3}, $\mu = 0.93$ cm^{-1}, and $T = 295$ K. Of the 3309 unique measured reflections, 2210 with $I > 3\sigma(I)$ were used in the refinement. R(on F) = 0.042, $R_w = 0.054$, and $S = 1.76$.

Crystal data for f: *o*-acetotoluidide, $C_{11}H_{13}NO_2$, $M_r = 191.23$, monoclinic $P2_1/c$ (no. 14), colorless, $a = 7.502(1)$, $b = 12.181(3)$, $c = 10.846(1)$ Å, $\beta = 100.44(1)°$, $V = 974.7(3)$ Å^3, $Z = 4$, $D_{calc} = 1.30$ g cm^{-3}, $\mu = 0.90$ cm^{-1}, and $T = 295$ K. Of the 2344 unique measured reflections, 1366 with $I > 3\sigma(I)$ were used in the refinement. R(on F) = 0.044, $R_w = 0.053$, and $S = 1.70$.

Crystal data for g: *o*-acetoacetanisidide, $C_{11}H_{13}NO_3$, $M_r = 207.23$, monoclinic $P2_1/a$ (no. 14), colorless, $a = 6.727(2)$, $b = 21.286(3)$, $c = 7.990(1)$ Å, $\beta = 113.70(2)°$, $V = 1074.6(4)$ Å^3, $Z = 4$, $D_{calc} = 1.31$ g cm^{-3}, $\mu = 0.96$ cm^{-1},and $T = 295$ K. Of the 2520 unique measured reflections, 1792 with $I > 3\sigma(I)$ were used in the refinement. R(on F) = 0.042, $R_w = 0.057$, and $S = 1.92$.

Spectroscopic Analysis. IR spectra were recorded on a Nicolet 510P FTIR spectrometer from KBr pellets and ^{1}H NMR spectra in $CDCl_3$ solution on a Gemini 300 Varian instrument.

Structural Data Retrieval. The search of the intramolecularly H-bonded fragments **II**−**V** was performed on the Cambridge Structural Database[12] (October 1998 release) on all structures having $R < 0.09$, σ(C−C) ≤ 0.008 Å, no disorder in the group of interest, and refined N−H hydrogens. Structures where a four- or five-membered ring was fused with two atoms of the enaminonic fragment were neglected because of producing unwanted changes in bond angles and abnormal H-bond distances. CSD reference codes were used to identify the 123 crystal structures retrieved in the Supporting Information.

Computational Details. The computational effort was particularly heavy because of the number and complexity of the molecules involved. The choice of a suitable level of theory was, therefore, crucial. It has been known since 1985[20a] that the H-bond geometries of RAHB molecules cannot be reproduced at the Hartree−Fock level. Conversely, geometry optimizations carried out by ab initio Møller−Plesset[25a,b] MP2 methods and a 6-31G(d,p) basis set (or larger) have yielded good agreement with experimental results for the O−H···O intramolecular RAHB of malondialdehyde,[20a,c] acetylacetone,[20b] 3-formylmalondialdehyde, and 3-formylacetylacetone.[20d] The problem of the basis set choice in strong H-bonds, also indicated as low-barrier H-bonds (LBHB)[2], has been investigated with some systematism by McAllister,[26] who concluded that "on the basis of geometric analysis, 6-31+G(d,p) is the best basis set for the general study of LBHBs", and that ab initio Møller−Plesset methods at the MP2, MP3, and MP4 level give very similar results among themselves and with respect to the density functional theory (DFT) methods B3LYP and BLYP.[25c−e] In view of these considerations and of the fact that DFT optimization is somewhat faster than the MP2 one, all calculations were accomplished by using the Gaussian 94[27] suite of programs at the B3LYP/6-31+G(d,p)//B3LYP/6-31+G(d,p) level of theory. The comparison between B3LYP and MP2 methods has been carried out for the parent β-enaminone molecule in its H-bonded (*cC*) and non-H-bonded (*tT*, *cT* and *tC*) conformations (Table 5) and shows that geometry and energy differences are barely relevant from a practical point of view.

In intramolecularly H-bonded molecules, the H-bond energy, ΔE_{HB}, can only be evaluated as the difference between the energies of the non-H-bonded (open) and H-bonded (closed) forms. For the simple β-enaminone (Table 5), there are three possible open isomers, which produce three different ΔE_{HB} values in the range of 4.4−7.6 kcal mol^{-1}. This number is severely reduced in substituted β-enaminones (Table 4), because open stereoisomers with strongly stabilizing interactions (such as H-bonds) or short destabilizing contacts give biased ΔE_{HB}

(25) (a) Here, W. J.; Radom, L.; Schleyer, P.v. R.; Pople, J. A. *Ab Initio Molecular Orbital Theory*; Wiley-Interscience: New York, 1986; and references therein. (b) Møller, C.; Plesset, M. S. *Phys. Rev.* **1934**, *46*, 618. (c) Kohn, W.; Becke, A. D.; Parr, R. G. *J. Phys. Chem.* **1996**, *100*, 12974. (d) Parr, R. G.; Yang, W. *Density Functional Theory of Atoms and Molecules*; Oxford University Press: New York, 1989. (e) Dreizler, R. M.; Gross E. K. V. *Density Functional Theory*; Springer: Berlin, 1990.

(26) (a) Pan, Y.; McAllister, M. A. *J. Mol. Struct.* (*THEOCHEM*) **1998**, *427*, 221. (b) McAllister, M. A. *J. Mol. Struct.* (*THEOCHEM*) **1998**, *427*, 39. (c) Smallwood, C. J.; McAllister, M. A. *Can. J. Chem.* **1997**, *75*, 1195.

(27) Frisch, M. J.; Trucks, G. W.; Schlegel, H. B.; Gill, P. M. W.; Johnson, B. G.; Robb, M. A.; Cheesman, J. R.; Keith, T. A.; Petersson, G. A.; Montgomery, J. A.; Ragjavachari, K.; Al-Laham, M. A.; Zakrzewski, V. G.; Ortiz, J. V.; Foresman, J. B.; Cioslowki, J.; Stefanov, B. B.; Nanayakkara, A.; Challacombe, M.; Peng, C. Y.; Ayala, P. Y.; Chen, W.; Wong, M. W.; Andres, J. L.; Replogle, E. S.; Gomperts, R.; Martin, R. L.; Fox, D. J.; Binkley, J. S.; Defrees, D. J.; Baker, J.; Stewart, J. P.; Head-Gordon, M.; Gonzalez, C.; Pople, J. A. *GAUSSIAN 94* (*Revision E.2*); Gaussian, Inc.: Pittsburgh, PA, 1995.

estimates and must be excluded. Because for compounds of Table 4 the less frequently hindered open conformer is *cT*, H-bond energies are given as $\Delta E_{HB}(cT)$ values because they are directly referred to the open *cT* form (**T3**−**T8**, **T14**, **T15**, **T20**, and **T23**), or relisted either to the open *tT* form without correction, because it mimics the *cT* one (**T10**−**T12**), or to the *tC* isomer (**T9**, **T13**, and **T16**−**T18**), which has been renormalized to the *cT* form by subtracting 2.38 kcal mol^{-1} = $\Delta E_{HB}(tC) - \Delta E_{HB}(cT)$ (Table 5). For compounds **T19**, **T21**, **T22**, **T24**, and **T25**, no H-bond energies were calculated because of lack of a suitable open configuration. All geometric optimizations were carried out in the C_s point group with the exception of the open form of **T14A** (Chart 1 and Tables 4 and S8), whose planar structure was heavily stressed and for which C_1 symmetry was adopted. The only molecules tested in both C_s and C_1 point groups were the four conformers of the reference enaminone **T3**, and no significant differences in geometry or energy were registered. H-bond energies so defined are to be corrected for the effects of zero-point vibrational energy (ZPC). For the sake of simplicity, this has been evaluated only for the B3LYP treatment of β-enaminone **T3** (Table 5), in which the corrected energies, ΔE_{HB}^{ZPC}, are, on average, 0.84 kcal mol^{-1} smaller than the uncorrected ones, and the Gibbs free energies, ΔG_{HB} are even smaller by approximately 0.61 kcal mol^{-1} because of the increased vibrational degrees of freedom of the open, not H-bonded, forms. Calculated N−H- and C═O-stretching frequencies (cm^{-1}) are also given in Table 5. $\nu_s(NH_2)$ is 3472 cm^{-1} for the H-bonded *cC* conformer with a decrease of approximately 153 cm^{-1} with respect to the average of the three non-H-bonded forms, which is in rather good agreement with experimental results (Figure 4a), as also is the corresponding shift from 1709 to 1744 cm^{-1}, on average, which was calculated for ν(C═O). Comparison to experimental frequencies[28] indicates that a reasonable matching can be achieved by multipying the calculated values of $\nu(NH_2)$ and ν(C═O) by 0.95. The N···O-stretching vibration is calculated to be 260 cm^{-1}. Its coupling with the N−H vibration is believed to produce the observed ν_{NH} broadening of approximately 500 cm^{-1} in H-bonded systems by the Stepanov mechanism.[4a]

(28) Colthup, N. B.; Daly, L. H.; Wiberley, S. E. *Introduction to Infrared and Raman Spectroscopy*, 3rd ed.; Academic Press: San Diego, CA, 1990.

Acknowledgment. This paper is dedicated to the memory of Prof. George A. Jeffrey, in acknowledgment of his great contribution to modern hydrogen-bonding studies. We thank Drs. F. Hernández-Cano and C. Foces-Foces (Instituto de Quimica Fisica 'Rocasolano', C.S.I.C., Madrid, Spain) for low-temperature crystallographic data collections and CINECA, Casalecchio di Reno (Bologna), for free use of its SG Origin2000 computing facility. This work was supported by the Italian Ministry for University and Scientific and Technological Research (MURST, Rome) and by the European Community Human Capital and Mobility Project (Contract ERBCHRX-CT940469).

Supporting Information Available: Tables of CSD[12] Refcodes, selected geometric parameters and Pauling's π-delocalization indices; table of IR ν_{NH} and NMR δ_{NH} data for compounds of known crystal structure; table of relevant energetic and geometric parameters for sample molecules optimized by quantum-mechanical DFT methods; tables of crystal data, structure solution and refinement, atomic coordinates, bond lengths and angles, and anisotropic thermal parameters for **a**−**g** (PDF); X-ray crystallographic file (CIF). This material is available free of charge via the Internet at http://pubs.acs.org.

JA000921+